Properties of Light mesons in the Nuclear Medium.

Chaden Djalali

University of South Carolina
Department of Physics and Astronomy
712 Main Street, Columbia, SC 29208, USA

ABSTRACT

The theory of the strong interaction, Quantum Chromodynamics (QCD), has been remarkably successful in describing high-energy and short-distance-scale experiments involving quarks and gluons. However, applying QCD to low energy and large-distance-scale experiments has been a major challenge. Chiral symmetry is one of the most fundamental symmetries in QCD and provides guiding principles to deal with strong interaction phenomena in the non-perturbative domain. Various QCD-inspired models predict a modification of the properties of hadrons in nuclear matter from their free-space values. A review of experiments searching for the in-medium modifications of light mesons will be given trying to assess if they confirm or refute these theoretical predictions. Several complementary high statistics experiments are planned at JLab, GSI, JPARC and RHIC to further study the properties of hadrons in the medium.

I – INTRODUCTION

In the current picture, ordinary matter represents only 4% of the total energy content of the universe and is made of leptons, quarks, and the particles that bind them (well described by the Standard Model). Hadrons, the strongly interacting particles are composite objects made of quarks and gluons. The dynamics of quarks and gluons is described by Quantum Chromodynamics (QCD) and manifests very peculiar properties.
For most composite systems, the total mass of the system is close to the sum of the masses of the constituents. The proton mass and the electron mass (almost) add up to the hydrogen-atom mass. Likewise, masses of two protons and two neutrons (almost) add up to the alpha-particle mass. The difference is the binding energy which compared to the total mass is of the order 10^{-8} for atoms and 10^{-3} for nuclei. However, this is not the case for hadrons. Under normal conditions, quarks are confined in hadrons. The masses of the u and d quarks are less than 10 MeV so naively one might expect the mass of the nucleon $m_{p,n}$ ~20-50 MeV. However, the observed mass of the nucleon is of the order of 1000 MeV.

Right after the Big Bang, quarks and leptons were mass-less. When the temperature of the universe dropped below 100 GeV, the spontaneous breaking of the electroweak symmetry resulted in Higgs particles condensing in the vacuum, this "Higgs mechanism" gave mass to leptons and quarks.[1] With further cooling, once the temperature dropped below 100 MeV, the quarks and gluons became confined in protons and neutrons. The QCD vacuum was modified by the spontaneous breaking of chiral symmetry giving the u and d quarks in the nucleon an "effective" mass of some 300 MeV/c^2.[2] This constituent mass of the quarks is different from their current mass. The Higgs mechanism is only

responsible for ~2% of the mass of the nucleon, QCD dynamically generates the remaining 98% of the mass of ordinary matter.
Experiments at the large hadron collider (LHC) at CERN are looking for the Higgs particle, the missing piece in the Standard Model. Many other experiments are carried out at different laboratories looking at the properties of hadrons and trying to describe them in terms of the fundamental degrees of freedom of QCD (quarks and gluons). This latter approach is successful at high energies/small distances but is still problematic at low energies/large distances. At low energies, standard nuclear physics with nucleon and meson degrees of freedom work effectively in describing observations. The transition between the two descriptions of hadrons is one of the main goals of hadronic physics. Lattice QCD calculations have made tremendous progress and will one day give us a full description of strong interactions under all regimes. Meanwhile, effective theories incorporating some of the main features of QCD have been successfully developed and help us gain insight into the non-perturbative regime of QCD. The study of the properties of hadrons in the medium provides stringent tests for these different models.

II – CHIRAL SYMMETRY AND QCD.

In QCD, the fundamental fields are the quarks (ψ_q) and gluons (A_ν) and their dynamics are described by the QCD Lagrangian. The gauge invariant QCD Lagrangian is:

$$L_{qcd} = i\sum_q \bar{\psi}_q^j \gamma^\mu (D_\mu)_{jk} \psi_q^k - \sum_q m_q \bar{\psi}_q^j \psi_q^k - \tfrac{1}{4} G^a_{\mu\nu} G_a^{\mu\nu} \qquad [1]$$

where the field strength tensor is:

$$G^a_{\mu\nu} = \partial_\mu A^a_\nu - \partial_\nu A^a_\mu + g f^{abc} A^b_\mu A^c_\nu \qquad [2]$$

The sum is over all the quarks u, d, s, c, b and t. D_μ is the covariant derivative acting on the quark fields, m_q is the current mass of the quarks and g is the coupling constant.
The QCD lagrangian exhibits a number of interesting properties. The most remarquable being that for an essentially "parameter free theory" it can account for the rich phenomenology of hadronic and nuclear physics. A simple approximation is to set the masses of the light quarks u, d and s to zero and those of the heavy quarks c, b and t to be infinite then the only parameter left in the QCD lagrangian is the running coupling constant g which is a function of the scale at which it is measured (Fig.1).

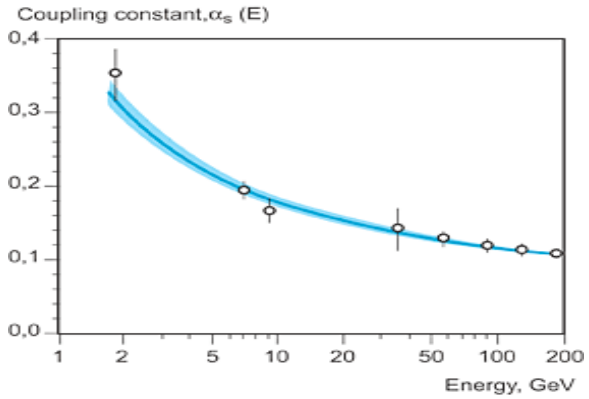

Figure 1: The value of the running coupling constant as a function of the energy scale E. The blue curve is a prediction of the asymptomatic freedom in QCD.

At low energies (large distances) the coupling constant is large but it decreases with increasing energy (short distances), this is the famous phenomenon of asymptotic freedom. [3]
A scale parameter $\Lambda_{QCD} \simeq 200$MeV ($\simeq$ 1 fm^{-1}) is introduced and in essence it is the scale at which the theory becomes non- perturbative.

Another important feature of the QCD lagrangian are its symmetries. First of all, the lagrangian is invariant under local gauge transformations. Furthermore if we consider only the light quark sector (u,d,s) and assume that $m_u=m_d=m_s$ then we have the well know flavor (isospin) symmetry of the strong interactions. This is a good symmetry in the light sector as observed by the degeneracy of isospin partner states. If in addition, we assume that the quark masses are equal to zero, then the flavor symmetry is enlarged. Left and right handed fields defined as $\psi_{L,R} = \frac{1}{2}(1 \pm \gamma_5)\psi$ do not couple to each other. The lagrangian is invariant under independent flavor transformations of the left and right handed fields. This corresponds to Chiral Symmetry and it is one the fundamental symmetries of QCD in the limit of mass-less quarks.

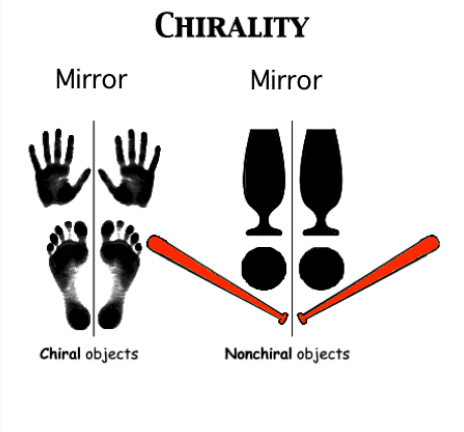

Figure 2 : Examples of chiral and non-chiral obiects

The concept of chiral symmetry was first introduced in 1884 by Lord Kelvin who wrote *"I call any geometrical figure, or group of points, chiral, and say it has chirality, if its image in a plane mirror, ideally realized, cannot be brought to coincide with itself."*[4]

For everyday object, this symmetry is easy to visualize (Fig. 2). Chirality plays an important role in chemistry and biology. All amino-acid molecules are chiral. We can only absorb sugars of definite chirality. Molecules with different chirality have different reactions: the well know sweetener aspartame has a specific chirality, its chiral partner is highly bitter.

For a moving particle with spin, the helicity is the projection of the spin onto its flight direction. For spin ½ particle, we have two states for the helicity: right handed (RH) and left handed (LH) (Fig.3). For a mass-less spin ½ particle, helicity and chirality are the same.

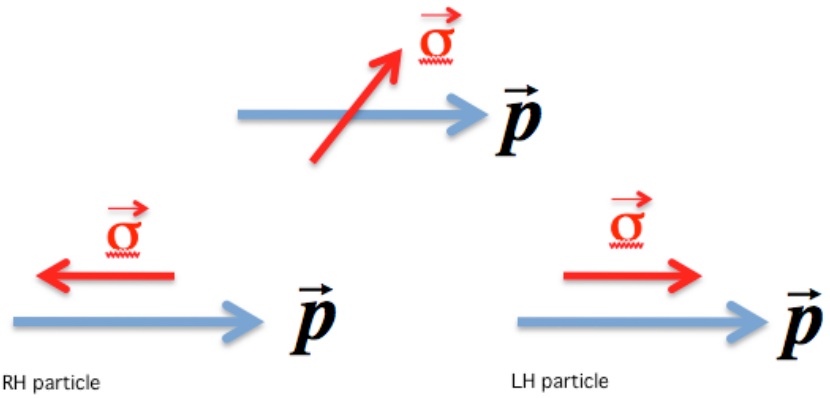

Figure 3 : Helicity states of a spin ½ particle

If we limit ourselves to the light quark sector and assume that the quarks are mass-less then we see that chiral symmetry becomes an exact symmetry of the lagrangian. It implies that we have $SU(n_f)_L \times SU(n_f)_R$ symmetry. The RH and LH quarks "don't talk to each other" and we expect chiral partners (pseudoscalar-scalar partners ; vector-axial partners,....) to be degenerate in mass.

In the real world the masses of up, down and strange quarks are not zero, nevertheless since $m_u, m_d << m_s < \Lambda_{QCD}$, one expects QCD to have an approximate chiral symmetry.

If we restrict ourselves to only u and d quarks, m_u, m_d (< 10 MeV) being relatively small, can be neglected (Fig. 4)[5] then we have an approximate chiral $SU(n_f)_L \times SU(n_f)_R$ symmetry. This is why low energy chiral effective theories are so successful.

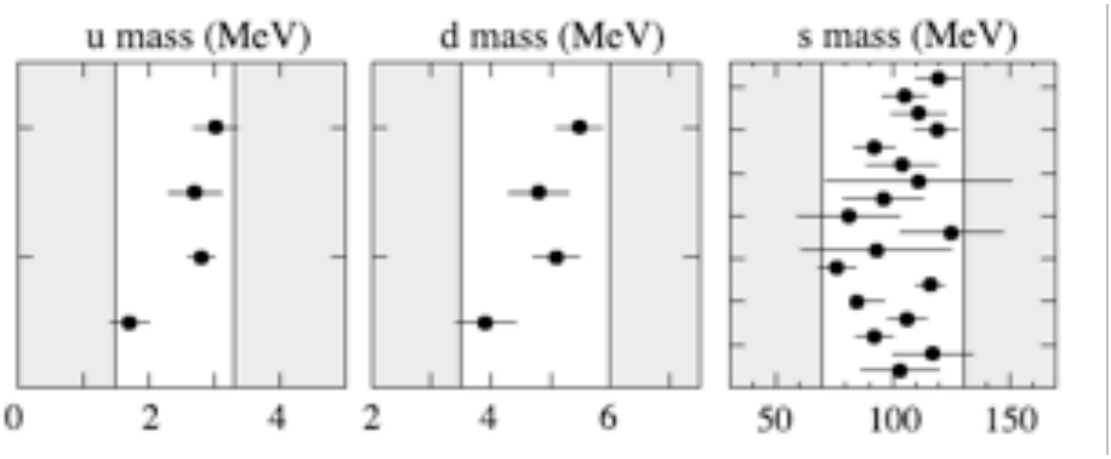

Figure 4 : Current masses of the u, d and s quark. The particle Data Group, 2008

Even if in the light quark sector, the QCD lagrangian is chiral invariant, the ground state (QCD vacuum) at zero temperature and density violates chiral symmetry. Chiral symmetry is spontaneously broken in the vacuum by the quark-antiquark condensate which mixes LH and RH quarks. This spontaneous breaking of the symmetry has important consequences for the dynamics of QCD at low energy. The Goldstone's theorem implies that the breaking is associated with the appearance of a octet of (approximately) mass-less pseudo scalar Goldstone bosons. The pion is a Goldstone boson. Its non-zero mass is due to the non-zero current masses of the up and down quarks. In the spontaneously broken state, the coupling to the quark condensates to the u and d quark , results in the "constituent mass" (~ 300 MeV/c²) of these quarks which is different from their current masses (~5-10 MeV/c²). This is shown by Lattice QCD calculations in figure 5.[6]

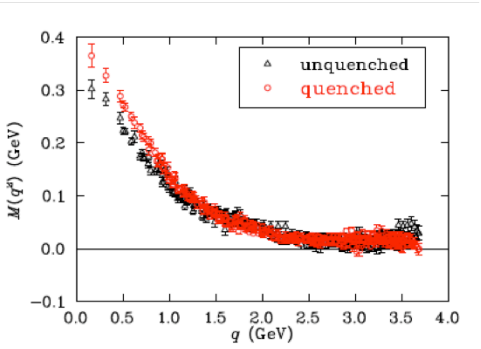

Figure 5 : Quark mass function LQCD calculations.

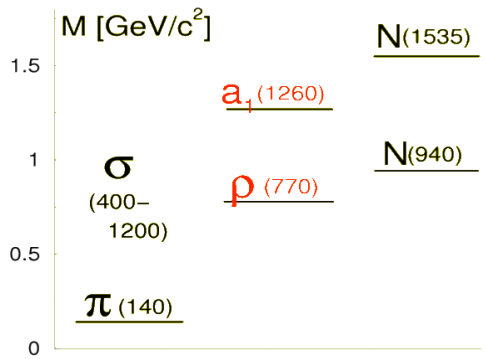

Figure 6 : Non-degeneracy of chiral partners

The broken chiral symmetry is also visible at the level of the low mass part of the hadronic spectrum where there is no degeneracy between possible chiral partners such as the pion and the sigma mesons, the rho and the a_1 mesons, and, the nucleon and N(1535) (Fig. 6). Experimentally the $\rho(770)$ meson is very different from the $a_1(1260)$ meson as observed in the τ-decay measured by the ALEPH collaboration (Fig.7).[7]

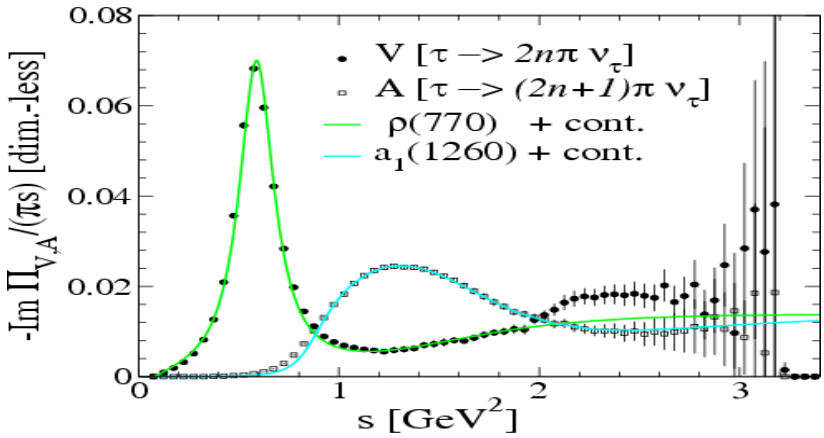

Figure 7 : The ρ and a_1 meson spectral functions observed in the τ decay by the ALEPH Collaboration.

In terms of the quark degrees of freedom, one order parameter measuring the violation of the symmetry is the quark anti-quark condensate which in the vacuum has a value of $\langle 0 | q\bar{q} | 0 \rangle \approx -(250\text{MeV})^3 \pm 10\%$. Another order parameter at the hadronic scale is the pion decay constant which is the vacuum is f_π ≈94 MeV. The pion decay constant f_π is related to the quark condensate $< 0 | q\bar{q} | 0 >$ by the Gell-Mann- Oakes – Renner (GOR) relation: [8]

$$m_\pi^2 f_\pi^2 = -2(m_u + m_d) < 0 | q\bar{q} | 0 > + O(m_q^q) \qquad [3]$$

It is predicted by LQCD and thermo-dynamical models that chiral symmetry is restored at high temperatures and/or densities. At full restoration of chiral symmetry, the order parameters are predicted to drop to zero.

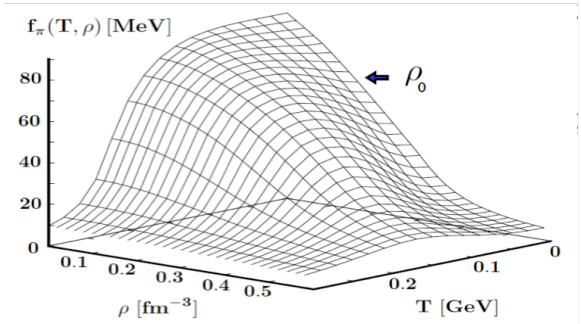

Figure 9 : Evolution of f_π as a function of T and ρ.

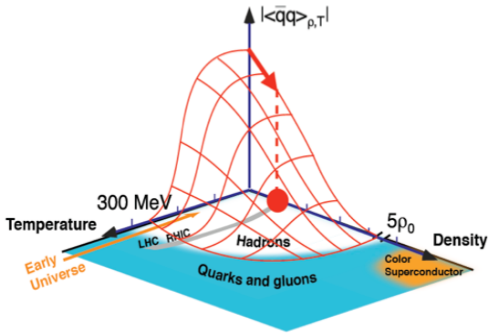

Figure 8:Evolution of $< 0 | q\bar{q} | 0 >$ as a function of T and ρ.

In Figures 9, one sees that at high enough T and/or ρ, the quark condensate $< 0 | q\bar{q} | 0 >$drops to zero.[9] At normal nuclear densities and T=0 (i.e. the center of a heavy nucleus) the condensate has dropped by almost 35%. This corresponds to partial restoration of chiral symmetry. The same behavior is predicted for the pion decay constant f_π in figure 8.[10] LQCD calculations also show that full chiral restoration coincides with deconfinement, although this is not fully understood.
Different theories predict that the magnitude of the condensate drops quadratically with the temperature and linearly with the density of the nuclear medium.[11]

$$\frac{f_\pi^2(T,\rho)}{f_\pi^2(0)} \approx \frac{<0|q\bar{q}|0>_{T,\rho}}{<0|q\bar{q}|0>_0} = 1 - \frac{T^2}{8f_\pi^2} - \frac{\sigma_N}{m_\pi^2 f_\pi^2}\rho + ... \qquad [4]$$

Another way of illustrating the breaking and restoration of chiral symmetry is in terms of an effective potential with two degrees of freedom, the pion and the sigma (scalar-isoscalar meson). In the vacuum, the potential has the shape of a Mexican hat (Fig 10.a) and the lowest possible state brakes the rotation symmetry in the π–σ plane. In this picture, the sigma corresponds to radial fluctuations of the amplitude of the condensate around the minimum of the effective potential. This requires energy, hence the larger

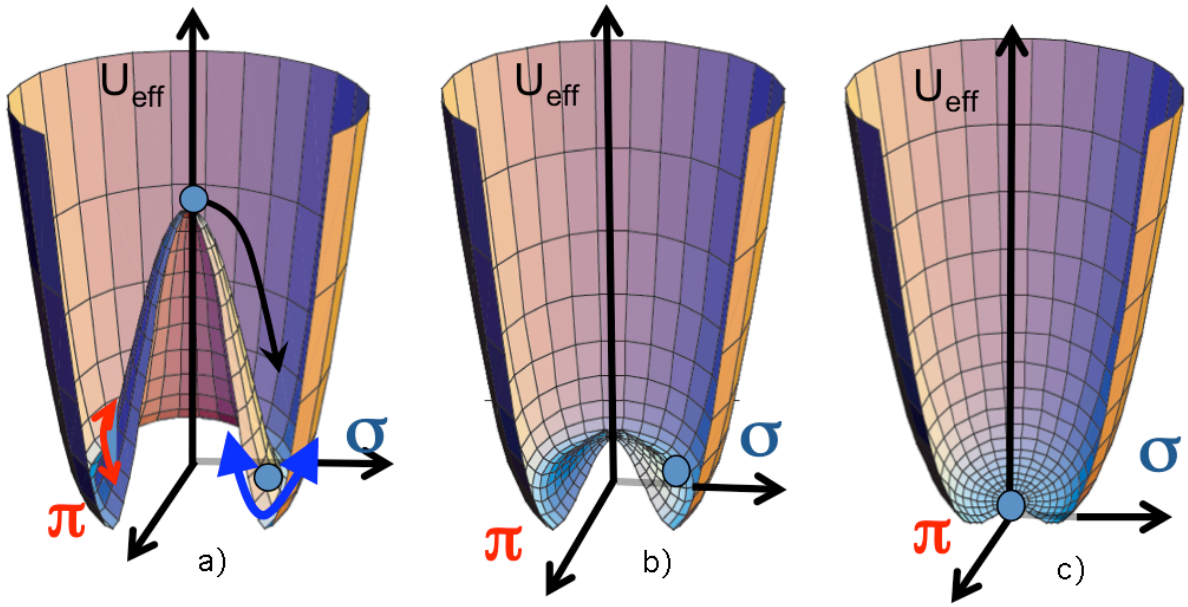

Figure 10 : Effective potential in terms of the pion and sigma degrees of freedom. Chiral symmetry is maximaly broken (a) ; partially restored (b); fully restored (c).

mass of the σ-meson. The pion corresponds to the phase-fluctuation, moving along the chiral circle at the bottom of the Mexican Hat potential. This doesn't require any extra energy, hence the almost mass-less pion. As chiral symmetry is gradually restored (Fig 10.b) the chiral circle shrinks and the mass of the sigma decreases until full chiral restoration where the potential has a parabolic shape. The potential being fully symmetric under rotations (Fig 10.c), the π and the σ have the same degenerate mass.

The study of chiral symmetry restoration is one of the main goals of hadronic physics. Contrary to the Higgs Boson, the quark condensate is not an observable. We need theoretical models to relate the quark condensate to actual experimental observations. The quark condensate is predicted to change in the nuclear medium, then it is natural to expect that the properties of the excited states (particles) which are created out of the vacuum state ("excitations of the QCD vacuum") will also change in the nuclear medium. Except for the pion, no simple connection between the condensate and the properties of the particle has been established. Some models, based on QCD, try to link the condensate to average properties of particles such as their masses. Several dynamical hadronic models, with different degrees of sophistication, calculate the spectral functions of hadrons in the medium,[12] providing much richer information than simple masses.[13,14] However, the link between spectral functions and actual observable is not straightforward.

III – MESONS IN THE MEDIUM - PREDICTIONS

There are many models predicting medium modifications of the properties of mesons in the medium. For more details see the comprehensive review by Hayano and Hatsuda.[15] We will briefly mention some of these models.
The constituent quark mass M originates mainly from the spontaneous breaking of chiral symmetry as proposed by Nambu and Jona-Lasinio (NJL) [16]. If we assume that the vector meson mass is just given by the additive rule, then it will be of the order of 2M. As chiral symmetry is restored, the constituent mass drops therefore one expects a drop in the mass of the vector meson. More elaborate models using the NJL approach at finite temperatures and density were proposed in the late 1980's[17] . Figures 11 and 12 respectively show the evolution of the order parameters and the masses of the mesons as a function of density.[18] The quark condensate and the pion decay constant drop with increasing density. It is interesting to note that the masses of the pion and the vector mesons are not changing with density. The spectral degeneracy between the π and the σ meson, the ρ and the a_1 meson occurs in dense matter where chiral symmetry is restored ($\rho \sim 4\text{-}5\ \rho_0$).

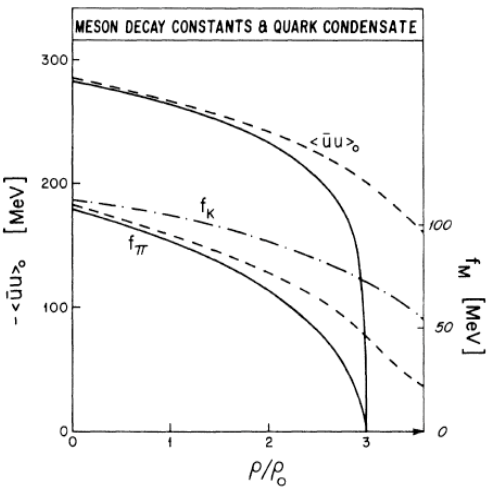

Figure 11: Quark condensate and pion decay constant as a function of density

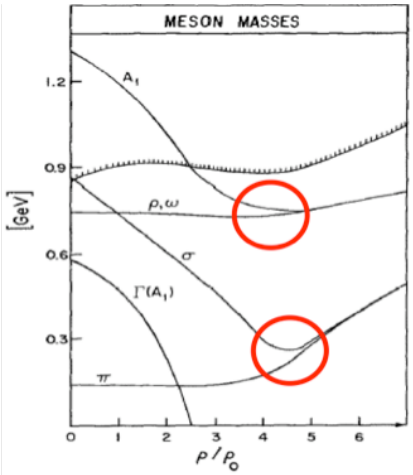

Figure 12: Evolution as a function of density of the masses of light mesons and their chiral partners.

The QCD sum rule method can relate the QCD condensate to the hadronic spectral functions. QCD sum rules in the medium provide useful constraints evaluating the weighted average of the spectral functions.[19] Hatsuda and Lee [20] have predicted that the mass of the vector mesons drops linearly (Figs.13 and 14) with the density as:

$$\frac{m_V^*}{m_V} = (1 - \alpha \frac{\rho}{\rho_0}) \qquad [5]$$

ρ_0 is normal nuclear density 0.17 fm^{-3}
$\alpha \sim 0.18 \pm 0.06$ for V= ρ ,ω
$\alpha \sim 0.15y$ for V= ϕ (y is the nucleon strangeness content)

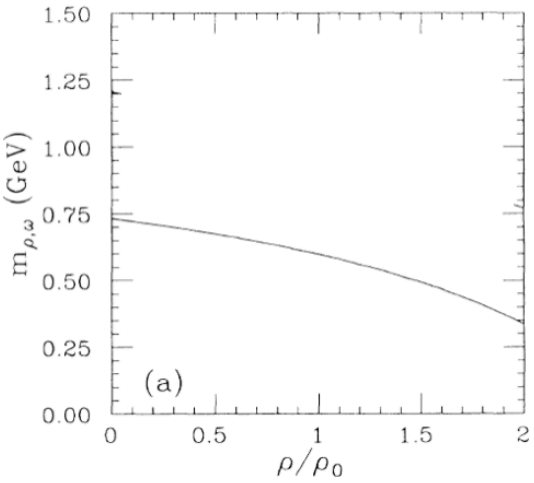

Figure 14: Mass of the rho and omega mesons as a function of density

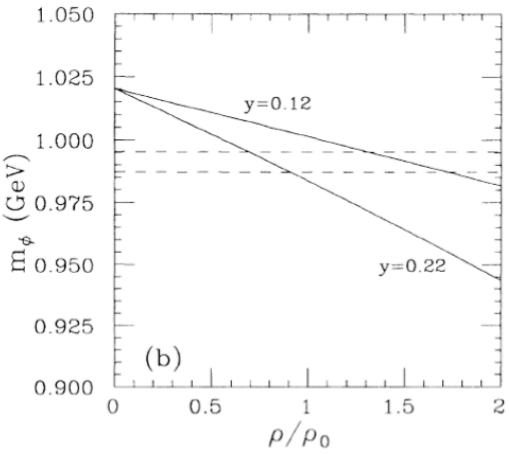

Figure 13: Mass of the phi-meson as a function of density

Brown and Rho [21] conjectured that the masses of light vector mesons (ρ, ω) scale universally as a function of density and/or temperature.

$$\frac{m_\sigma^*}{m_\sigma} \approx \frac{m_N^*}{m_N} \approx \frac{m_\rho^*}{m_\rho} \approx \frac{m_\omega^*}{m_\omega} \approx \frac{f_\pi^*}{f_\pi} \approx 0.8 \left(\rho \approx \rho_0 \right) \qquad [6]$$

Theoretical foundations for such scaling (called Brown-Rho scaling) were shown using effective chiral lagrangians with scaling properties of QCD leading to approximate in-medium scaling law.[22]

The Quark-meson coupling model (QMC), is a phenomenological theory in which quarks and gluons are confined in a "bag" inside non-perturbative QCD vacuum. In the medium, baryons composed of three valence quarks feel both scalar and vector potentials with opposite sign, while the mesons composed of quark and anti-quark only feel the scalar potential and obey a universal scaling law (Fig. 15).[23] It is interesting to note that at normal nuclear density (ρ_0), the ρ and ω -masses have dropped by ≈ 15%; the Nucleon-mass has dropped by ≈ 20% and the D-meson mass has dropped by ≈ 3%.

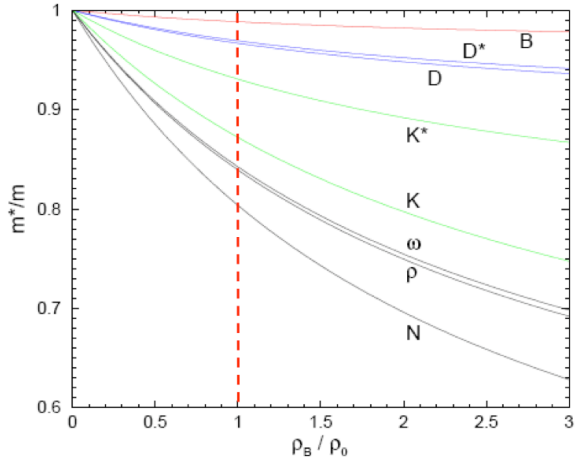

Figure 15: QMC model predictions for the evolution of the masses of hadrons as a function of density.

Hadronic models use a purely hadronic description of the mesons in the medium. The in medium self energy of the meson receives contributions from the low-energy particle-hole (p-h) excitations and the high energy nucleon–antinucleon excitations (Fig 16).

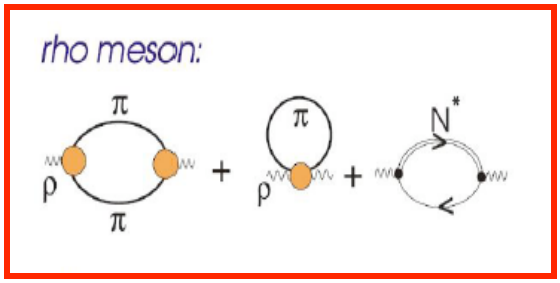

Figure 17: The ρ-meson propagating in the medium (hadronic models).

As it propagates in the nuclear matter, the vector meson feels not only the nucleon excitation but also the resonance excitations such as Δ and N∗. These models provide much "richer" information about the in-medium properties of the mesons. The spectral functions are modified in non-trivial manners such as spectral shifts, spectral broadening and new spectral peaks. Figures 17 and 18 show the predictions of different hadronic models for the ρ and ω mesons.[24]

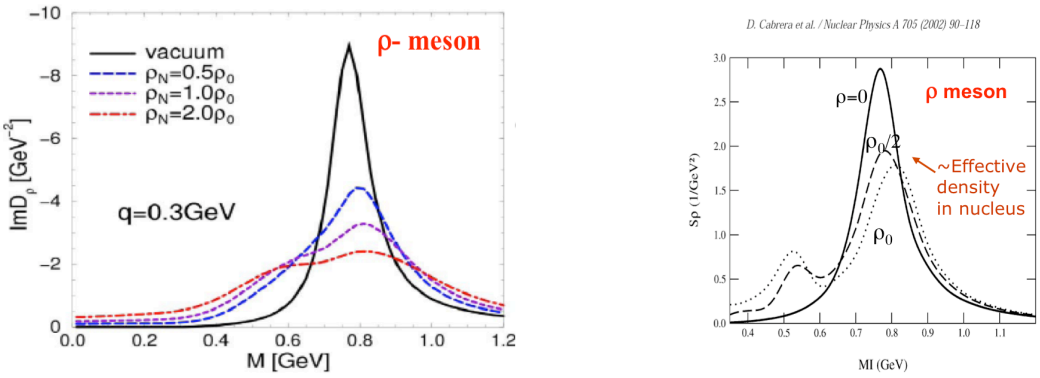

Figure 16: The ρ-meson spectral functions as a function of density.

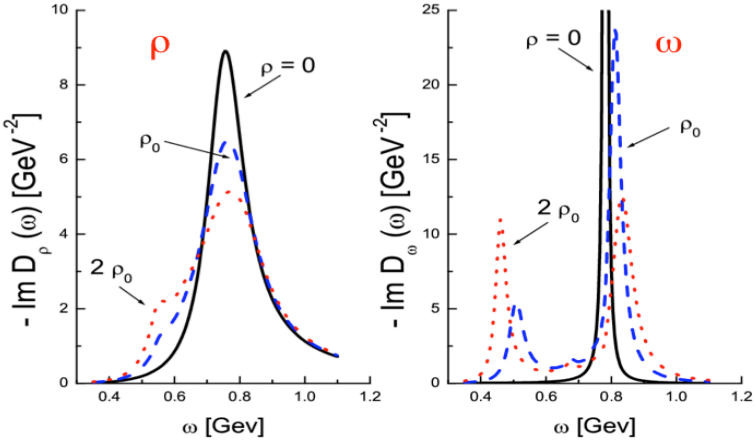

Figure 18: Spectral functions of the ρ and ω mesons as a function of density

As mentioned previously, one of the best indications of chiral symmetry restoration is the spectral degeneracy of chiral partners. In the light meson sector, the σ and the π mesons

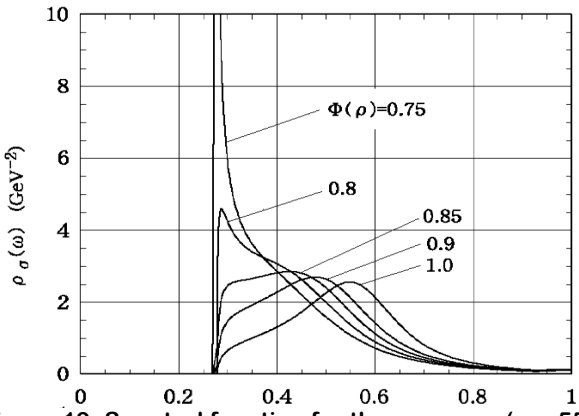

Figure 19: Spectral function for the σ- meson (m_σ=550 MeV).

should end up having the same mass. An interesting prediction is the spectral enhancement in the scalar-isoscalar channel (σ meson) near the 2π threshold at finite baryon density (Fig. 19).[25]

All these models make measurable predictions even at normal nuclear densities (mass shift, change in interaction, widening, extra peaks, etc.). For now, these effective theories are the best we have until LQCD calculations produce reliable results at finite density and temperature.

Experimentally, one needs to measure and compare the properties of these hadrons in the vacuum and in different media (T and/or $\rho \neq 0$) as illustrated in Figure 20.

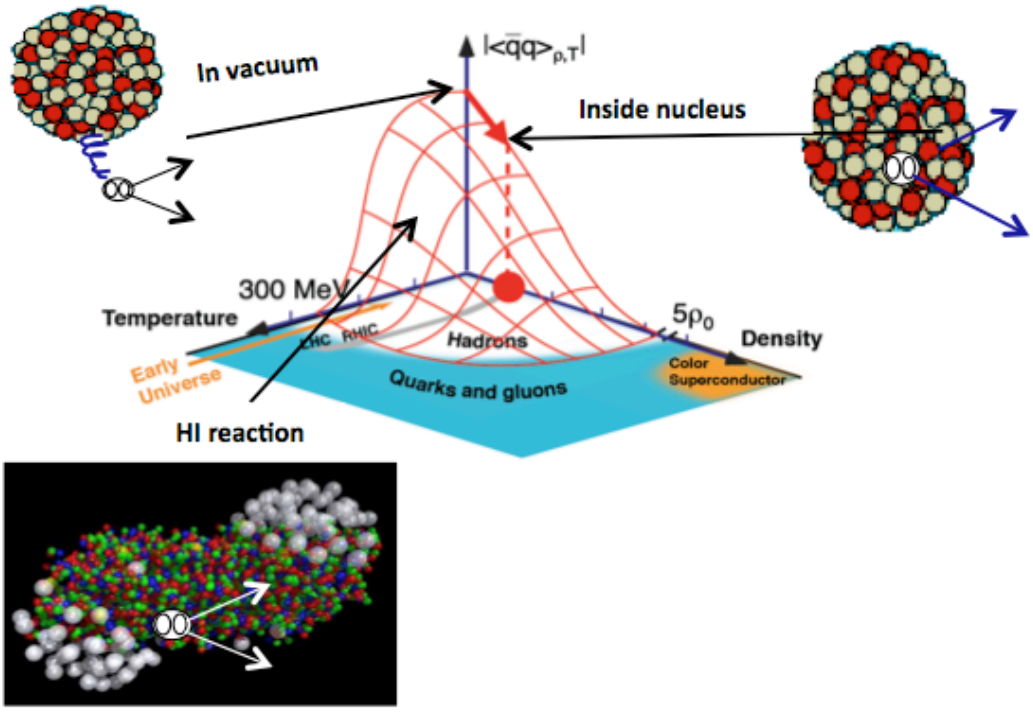

Figure 20: Mesons as probes of Chiral Symmetry restoration. Studying meson properties in the vacuum (T=0, ρ= 0), in the nucleus (T=0, ρ= ρ_0) and in heavy ion reactions (T>0, ρ) sheds light on possible restoration of chiral symmetry.

The experiments roughly fall under two categories.

1) Looking at the modification of the meson-nucleon interaction in medium such as in pionic states in nuclei, in elastic pion-nucleus scattering at low energy, in double pion production and kaon production in nuclei.
2) Looking at the modification of the mass and width of light vector mesons ρ, ω and φ in relativistic heavy ion collisions and in nuclei.

IV – PIONS AND KAONS IN THE MEDIUM – EXPERIMENTAL RESULTS

As we saw in the introduction, the chiral condensate in nuclear matter is predicted to drop by almost 35%. The GOR relation (equation 3) links the chiral condensate to the mass of the pion and its decay constant. Since the pion is a Goldstone boson, its mass is not expected to change dramatically with increasing nuclear density therefore a drop in the quark condensate should result in a drop in the pion decay constant. A possible way to look for this reduction is to study the in-medium pion properties through the precision spectroscopy of deeply bound pionic atoms and through the precision measurement of the low-energy pion-nucleus scattering.

Pionic Atoms

The first studies of bound pionic atoms were down by captured π^- in atomic orbits and measuring transitions by X-ray spectroscopy. To "feel the medium", the π needs to be in lowest orbits (1s, 2p). In Pb that is not possible, the last observed transition is: 4f → 3d.[26]

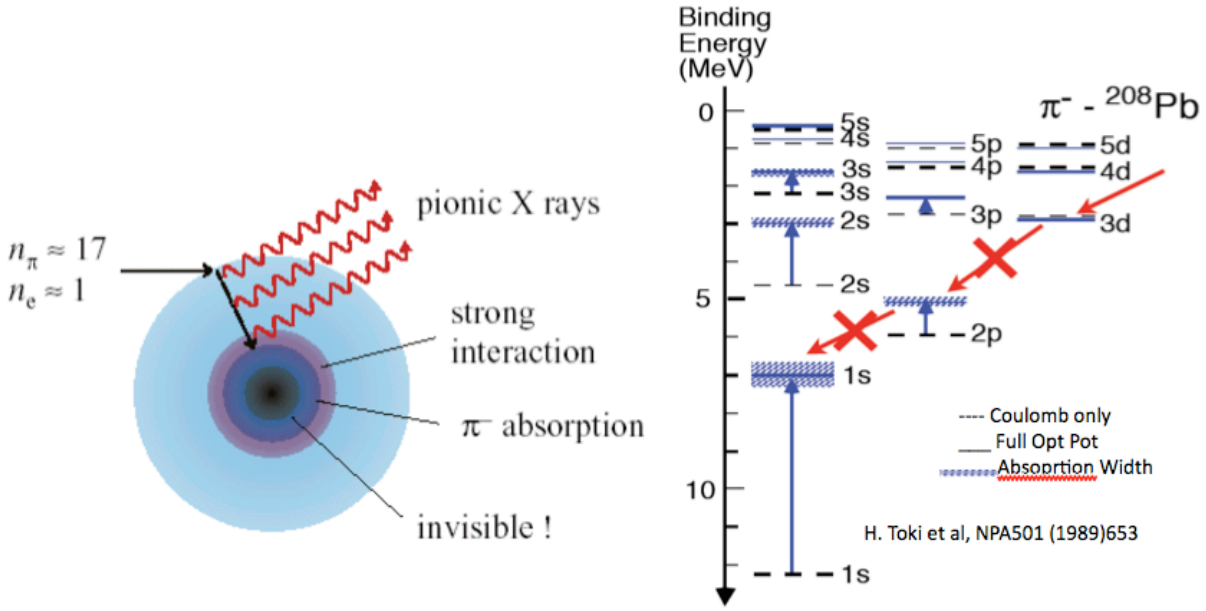

Figure 21: Limits of X-ray spectroscopy due to absorption of the pion before reaching deep orbits where the effect of the medium is felt.

A solution around this problem was proposed by Toki and Yamazaki[27] and consisted in trying to "deposit the pion" in the deep orbits by nuclear reactions. In the 1s orbit, the wavefunction of the π^- bound to a heavy nucleus overlaps appreciably with the nuclear density distribution, therefore the in-medium modification of the pion properties may have detectable effects on the binding energy and/or width of the bound state.
The first attempt looking at these deep bound states was done at TRIUMF the ^{208}Pb(n, p) reaction but no bound state was observed.[28] Soon after, it was suggested that recoilless reactions such as proton pick-up pion transfer (n,d) or (d,^{3}He) would be better suited to reach the deep orbits.[29] In 1996, the S160 experiment at GSI succeeded in observing the 2p and 1s states of pionic ^{207}Pb using the ^{207}Pb (d,^{3}He) reaction firmly establishing the methodology of deeply bound pionic atom spectroscopy.[30]
The S236 experiment at GSI, a follow-up experiment to S160, measured the 1s binding energies and widths of $\pi^- \otimes^{115,119,123}$ Sn using the ^{116,120,124}Sn(d,^{3}He) reactions (Fig 22).[31] The wide range of Sn isotopes and the good resolution has allowed a good determination

of the in-medium isovector scattering length b_1. The isovector scattering length in vacuum was precisely measured in pionic hydrogen measurement at PSI.[32]

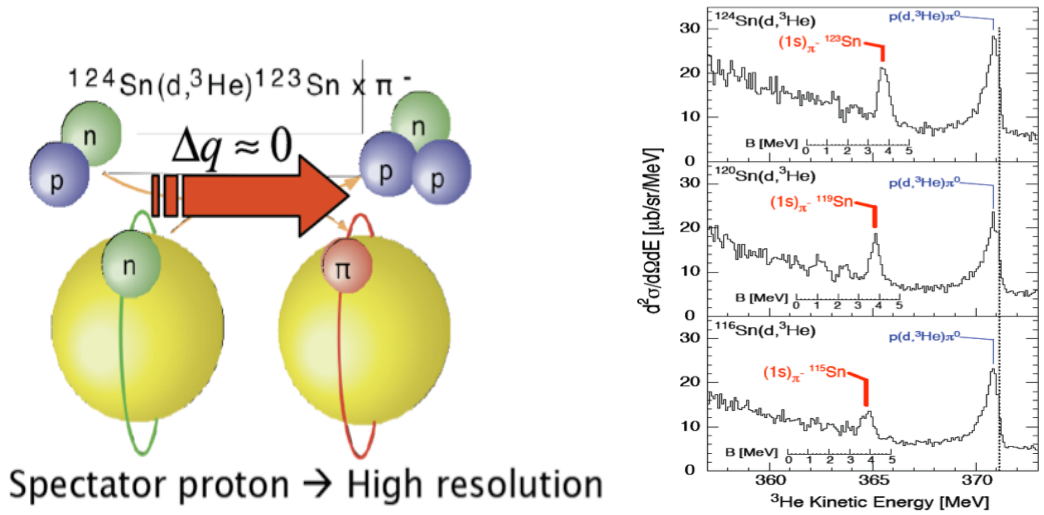

Figure 22: S236 experiment at GSI-FRS. In the recoilless experiment, the deep bound pionic 1s states are clearly observed for the first time in Sn isotopes.

From the measured binding energies of the deeply bound states, one can derive the value of the in-medium isovector scattering length b_1, the in-medium pion decay constant and the in-medium quark condensate. The steps are shown in figure 23 (from Hayano[33]).

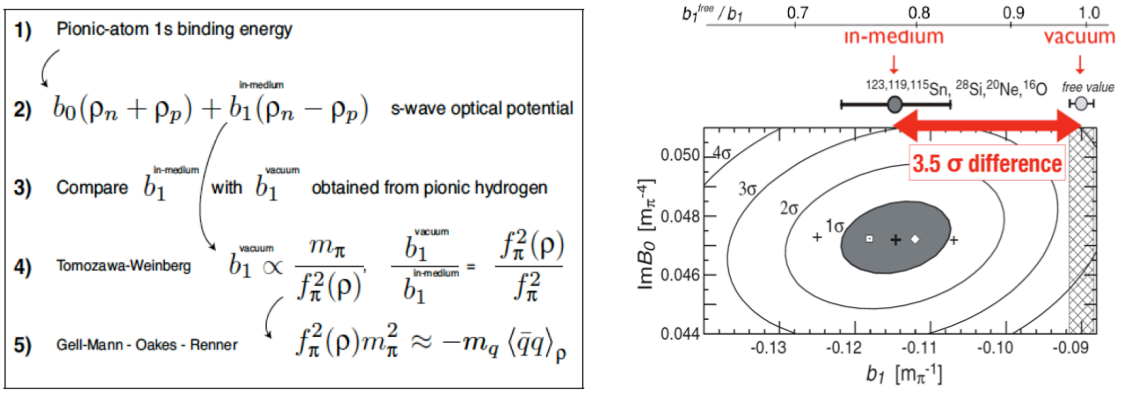

Figure 23: Steps from the measured binding energy to the quark condensate in deeply bound pionic atom spectroscopy (left). In medium isovector scattering length measured in Sn isotopes.

The current best result is that in the Sn isotopes ($\rho_{effective} \sim 0.6\ \rho_0$) the ratio of b_1 in vacuum to b_1 in the medium is 0.78 ± 0.05 corresponding to a drop of almost 35% of the quark condensate at normal nuclear density ρ_0:

$$\frac{<0|q\bar{q}|0>_{\rho_0}}{<0|q\bar{q}|0>_0} \approx 0.67 \qquad [7]$$

So far, this is the best experimental evidence for partial restoration of chiral symmetry in nuclear matter. These results are sensitive to the neutron skin radius and more precise

experiments are planned at RIKEN. Extensive theoretical work is also underway trying to determine higher order corrections to the in-medium Tomozawa-Weinberg and GOR relations.

Low energy π-nucleus elastic scattering

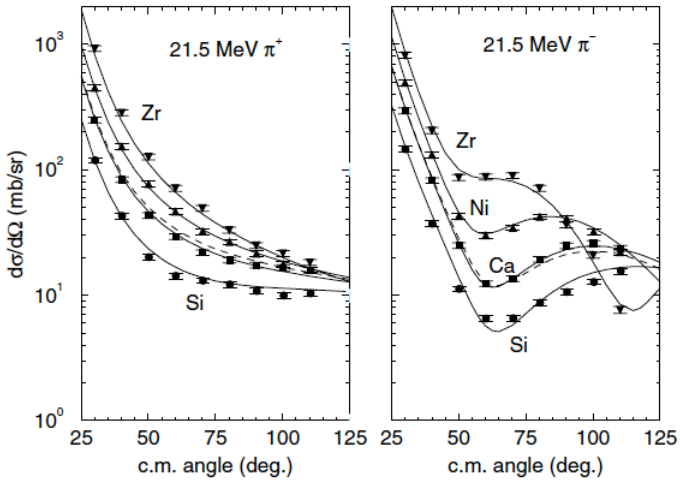

Figure 24: Elastic scattering of low energy pions at PSI

The classical approach to investigate optical potentials and derive the in-medium scattering lengths are complementary experiments to the deeply bound pionic atom studies. Elastic scattering positive and negative pions of 19.5 and 30 MeV from ^{40}Ca at LAMPF[34] and 21.5 MeV from Si, Ca, Ni and Zr at PSI (Fig 24)[35] allows a determination of the in-medium isovector scattering length and is consistent with deeply pionic bound state results, f_π^2 is reduced by 22 % at $\rho \sim 0.6\ \rho_0$ corresponding to a drop of 37% of the quark condensate.

Double pion production and the sigma meson

The scalar-isoscalar σ-meson has been a very elusive "particle". In the particle data book it is identified as the $f_0(400\text{-}1200)$ with a width of 400-500MeV. This large natural width in free space makes it doubtful that this particle is a mesonic state, and there has been many discussions on its nature. it has been long debated whether there exist unambiguous experimental evidences of such a light and broad resonance in the $\pi - \pi$ scattering, the $\gamma - \gamma$ collision, heavy meson decays.[36] Recent analysis seem to indicate that the σ definitely exists with a mass of the order of 500 MeV and a width of the order of 500 MeV.[37] Although the existence of σ is established, its quark gluon structure is still unknown and is actively studied theoretically, experimentally.
The σ-meson has the same quantum number as the vacuum and is interpreted as amplitude fluctuations of the quark condensate. Its properties are expected to change in the medium closely following the changes in the condensate. As seen in Figure 19, an interesting prediction is an enhancement in the I=0, J=0 two-pion channel close to the 2-π threshold.

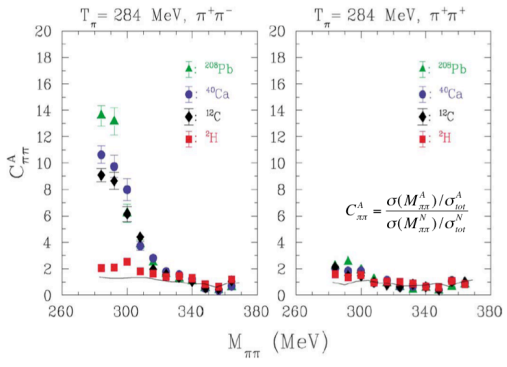

Figure 25: CHAOS experiment results.

The 2-π production on nuclei has been studied with pion and photon beams. In photo-production reactions, larger effective densities are probed (2/3 ρ_0) as compared 1/3 ρ_0 with pion beams.
The CHAOS experiment TRIUMF using pions beams with energies in the range 240-305 MeV on ^{2}H, ^{12}C, ^{40}Ca and ^{208}Pb, observes a substantial enhancement of correlated pions in $\pi^+\pi^-$ close to $2m_\pi$ threshold for heavy nuclei. No enhancement is observed in the $\pi^+\pi^+$ channel (Fig. 25).[38]

The Crystal Ball (CB) collaboration at the AGS has studied the $\pi^0\pi^0$ channel on CH_2, CD_2, C, Al and Cu with a π^- beam.[39] The results on C are consistent with CHAOS results (only common target).

The two-pions channels ($\pi^0\pi^0$, $\pi^0\pi^+$, $\pi^0\pi^-$) have been studied in a photo-production experiment at the MAMI facilty using the TAPS spectrometer. Differential cross sections have been measured for several nuclei (^{1}H,^{12}C, and Pb) with tagged incident-photon of energies in the range of 400–460 MeV. A significant nuclear-mass dependence of the $\pi^0\pi^0$ invariant-mass distribution is found in the *I=0, J=0* channel. This dependence is not observed in the other two-pions channels (Fig 26).[40]

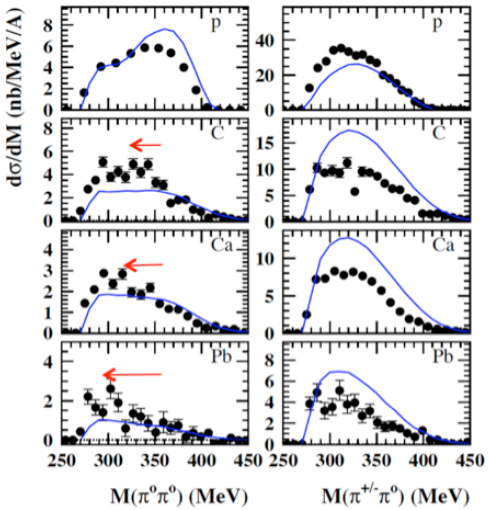

Figure 26: TAPS results

Although the observed enhancements seem consistent with a moving of the σ pole to lower masses and widths as the nuclear density increases, one has to be careful before concluding anything about chiral restoration since semi-classical Boltzmann-Uehling-Uhlenbeck (BUU) calculations without any medium effects reproduce the data reasonably well.[41] It seems that important contributions to the "softening" of the $\pi^0\pi^0$ spectra come from charge-exchange pion-nucleon scattering, which mixes the contributions from the different charge channels. Final state interactions dominate and one cannot conclusively say anything about restoration of chiral symmetry and medium changes of the σ-meson.

Kaons in the medium

We will not cover here the very active field of kaonic atoms but look at the production of kaons in nuclei. Theoretical models[42] predict sizeable medium modifications of masses and coupling constants for kaons and antikaons. As density increases, $m_{eff}(K^+)$ rises slightly while m_{eff} (K^-) drops "fast". Kaons (K^+,K^0) feel a weak repulsive potential, while anti-kaons (K^-,K^0) feel a strong attractive potential. This can lead to the condensation of anti-kaons in dense baryonic matter such as in neutron stars.[43]

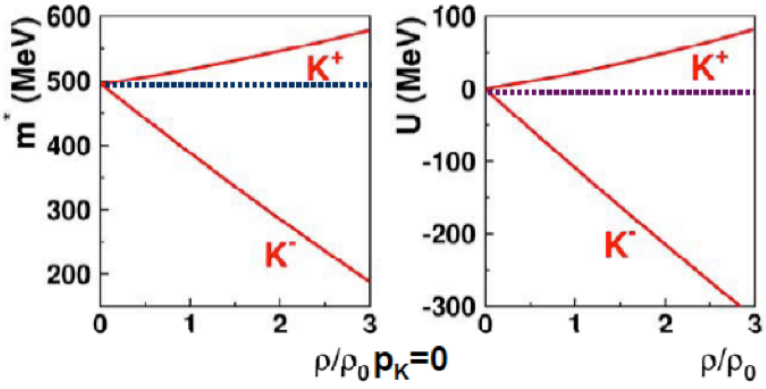

Figure 27: Medium modification of the mass and interaction of kaons as a function of density.

Quark-meson coupling (QMC) calculations[44] predict that Kaons (K^+, K^0) and hyperons (Λ, Σ) are produced via the formation of intermediate Δ and N* resonances which are modified in the medium leading to substantial changes of the kaon production cross sections at normal nuclear matter density.

The FOPI collaboration at GSI has measured the in-medium K^0 inclusive cross sections in A(π^-, $\pi^+\pi^-$)X on C, Al, Cu, Sn and Pb with a pion beam having a momentum p_π=1.15 GeV/c].[45]

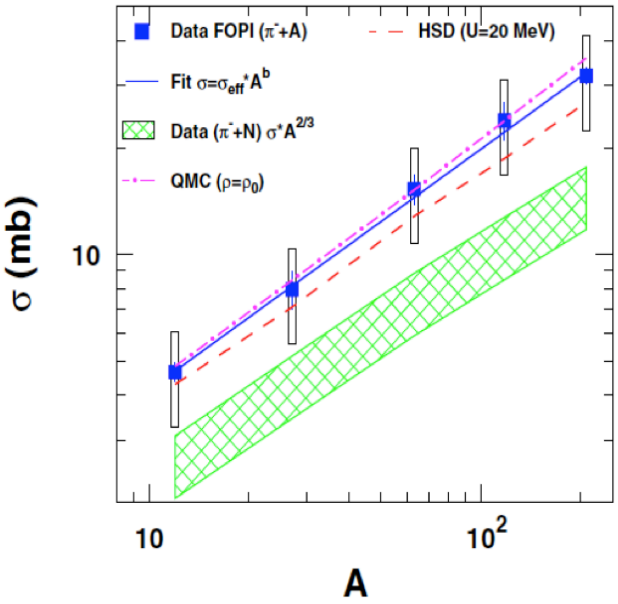

Figure 28: The inclusive K^0 cross section as a function of the target nucleus A.

The mean free path of 1 GeV/c kaons in nuclear matter is of the order of 1 fm. The kaons ar expected to be producted on the surface of the nucleus.
The FOPI data are fitted by a power law using an effective cross section (Fig.28):

$$\sigma = \sigma^{eff} A^b$$

with $\sigma^{eff} = 0.87 \pm 0.13\ mb$, and

$$b = 0.67 \pm 0.03$$

The slope parameter is consistent with 2/3 which indicates that the incoming π^- are absorbed at the nucleus' surface.
The hatched area in Fig. 28 is the expected cross section as scaled from the elementary reaction (Eq. 8) by the found A dependence. The data points are significantly above this expectation, which points to an in-medium modification of the cross section when going to nuclear targets.

$$\sigma^{eff} = \frac{Z}{A}\left[\sigma(\pi + p \to K^0 + \Lambda) + \sigma(\pi + p \to K^0 + \Sigma^0)\right] + \frac{N}{A}\left[\sigma(\pi + n \to K^0 + \Sigma^-)\right] \qquad [8]$$

The QMC model fits the trend, but this is strange since the effective density probed here is of the order 0.6 ρ_0 and QMC prediction are for nuclear matter at ρ_0. The Hadron-String Dynamics (HSD) transport code can be directly compared to the data.[46] The conclusion is that the inclusive total cross section is not sensitive to the modification of K-N in the medium. However, the ratio of kaons yields as a function of momentum in the laboratory shows sensitivity to the medium (Fig. 29).

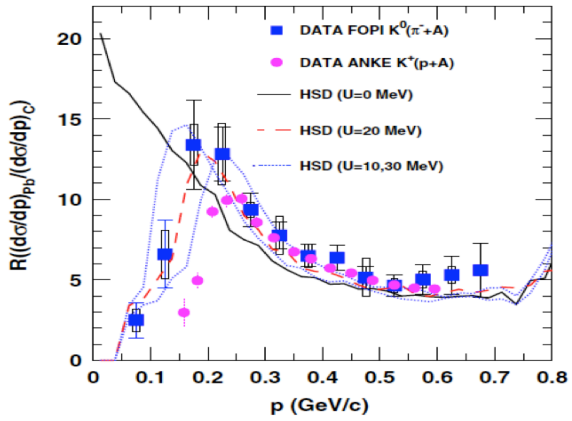

Figure 29: Ratio of yields for K0 (K+) produced by pions (protons) on Pb and C seen in FOPI (ANKE) as a function of the kaon momentum. The lines represent HSD transport code calculations with different depths of the in-medium potential.

The ANKE collaboration at COSY has measured the in-medium K^+ inclusive cross sections in A(p, K^+)X, (A=Cu, Au; E_p=2.3 GeV).[47]

At momenta p > 250 MeV/c, the FOPI and ANKE ratios agree. K^0s with momenta p < 170 MeV/c are suppressed in Pb with respect to C. Same pattern Is observed for K^+ with momenta p<250 MeV/c.
A repulsive KN potential in the nuclear medium can explain this observation. The kaons are accelerated before getting out of the nucleus. The larger the nucleus , the longer the kaons feel the Coulomb repulsive potential, increasing the depletion for K^+.
The HSD transport model calculations show sensitivity to these ratios. A repulsive KN potential of 20 ± 5 MeV (at normal nuclear density) explains the FOPI and ANKE results.

V – VECTOR MESONS IN THE MEDIUM – EXPERIMENTAL RESULTS

Many experiments have been studying the properties of the light vector mesons ρ, ω and ϕ in the medium, using simple probes such as γ, π or p on nuclei (T=0 and $\rho \sim \rho_0$) or in relativistic heavy ion collisions (T and/or $\rho > 0$). Sizeable modifications of the properties of these mesons are predicted even at normal nuclear densities. Table 1 lists the properties of the light vector mesons.

Properties of Vector Mesons $J^p=1^-$ (PDG-2008)						
Meson	Mass (MeV/c^2)	Γ (MeV/c2)	$c\tau$ (fm)	Main decay	$\Gamma_{e^+e^-}/\Gamma_{tot}$ ($x10^{-5}$)	$\Gamma_{\mu^+\mu^-}/\Gamma_{tot}$ ($x10^{-5}$)
ρ	775.49 ±0.34	149.4±1.0	1.3	$\pi^+\pi^-$ (~100%)	4.7	4.6
ω	782.65 ±0.12	8.49±0.08	23.2	$\pi^+\pi^-\pi^0$ (89%)	7.2	9.0
ϕ	1019.45 ±0.02	4.26±0.04	46.2	K^+K^- (49%)	3.1	3.2

Table 1: Light Vector mesons ρ, ω and ϕ the particle data book (2008).[5]

From Table 1, one sees that the ρ meson has a very short lifetime leading to the largest probability of decaying in the medium, while the ω and φ mesons will mostly decay outside the medium in which they are produced. In order to study their in-medium properties, it is crucial to choose a proper reaction allowing the observation of slow moving ω and ϕ mesons. The most interesting property of these vector mesons is that they decay into di-leptons which have negligible final state interaction (as illustrated in Fig. 30), allowing a "clean reconstruction" of the decay vertex.

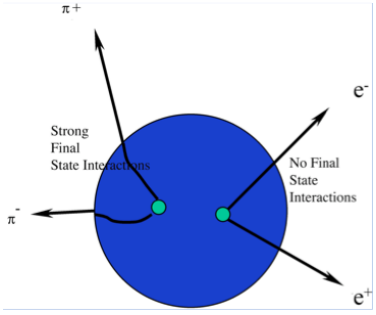

Figure 30: Final state interaction for pions and electrons

However, measuring the di-lepton spectra is very challenging because of the very small branching ratio (~10^{-5}) for this decay channel. Further complications come form the fact that there are hadronic sources which can produce leptons. One must have:

1) an excellent lepton-hadron discrimination capability;
2) the ability to suppress the huge combinatorial background (severe problem in heavy ion collisions);
3) the ability to account for all other physics channels producing to di-leptons,.

-Lepton-hadron discrimination

Detecting $\mu^+\mu^-$ final state.

Muons from pion and kaon decays are orders of magnitude more abundant than those from the vector meson decay into $\mu^+\mu^-$. It is therefore essential to have a thick absorber as close as possible to the interaction area to absorb as many pions and kaons as possible. Figure 31 shows in a schematic form the main set-up for experiments detecting muon-pairs. Multiple scattering and energy loss in the absorber (especially for low energy

muons) affects the invariant mass resolution. Magnetic spectrometer are needed for measuring the momentum of the muon.

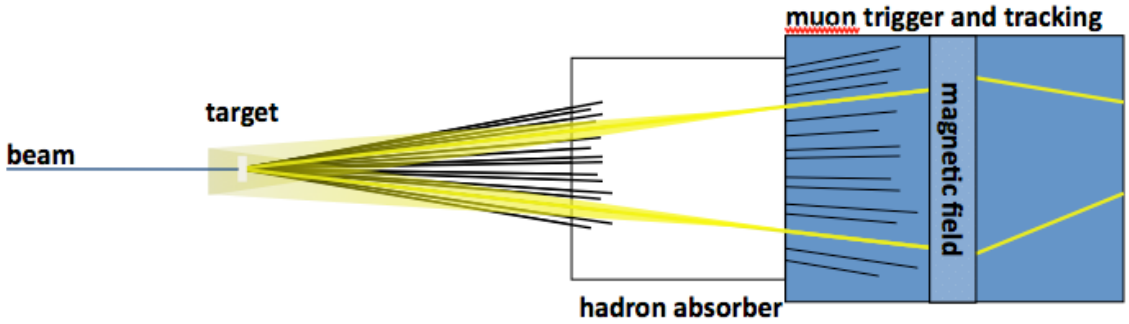

Figure 31: Schematics of typical muon detection system (NA60, ALICE,…)

Detecting e^+e^- final state.

An excellent electron identification is needed to get the electrons out of the huge hadronic background. A π-e discrimination of the order of at least 10^{-3} is required (π-pair suppression ~10^{-6}). This is achieved with a combination of Cerenkov detectors (either standard Cerenkov or ring imaging Cerenkov) and electromagnetic calorimeters.
A magnetic spectrometer is used to measure the momentum of the electrons and positrons. The momentum measurement directly affects the invariant mass resolution. Minimizing high-Z materials in the path of the beam, helps to drastically reduce the unwanted electromagnetic background. If solid targets are used, they are generally made of thin multilayer targets in order to reduce multiple scattering of the outgoing electrons/positrons.

The combinatorial background

The combinatorial background is the random combination of pairs of leptons (l^+l^-, l^-l^-, and l^+l^+) due to the uncorrelated sources. Figure 32 shows possible e^-, e^+ combinations.

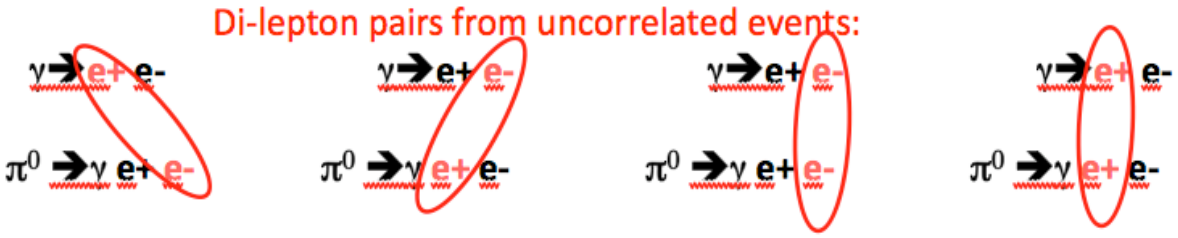

Figure 32: Possible random combinations leading to the combinatorial background in e^-, e^+ experiments .

In almost all of the experiments, the combinatorial background (CB) is severe, especially in high energy relativistic heavy-ion collisions (Table 2). In the case of the PHENIX experiment at RHIC, the ratio of signal to combinatorial background is of the order of 1/100![48]

experiment	NA60	PHENIX	NA45	HADES	KEK	TAPS	JLab
Signal/CB	1/11	1/100	1/22	~1/10	1/2 - 1	0.7-1	2-3

Table 2: Ratio of signal to Combinatorial background (CB) in different experiments

In spite of the small signal-to-background ratios, methods such as event mixing and like-sign pair subtraction have been developed to reliably subtract the background and extract meaningful results. Pairs of identical leptons (e^+e^+, e^-e^-, $\mu^+\mu^+$, $\mu^-\mu^-$), which are only produced by uncorrelated processes, will provide both the normalization and shape of the actual combinatorial background (CB). If enough same sign pairs are measured, then in each invariant mass bin :

$$Signal = N_{+-}^{meas} - CB = N_{+-}^{meas} - 2\sqrt{N_{++}^{meas} N_{--}^{meas}} \qquad [9]$$

if same acceptance for + and – charges. If the acceptances for different charges are not the same, then using the acceptances A_{+-}, A_{++} and A_{--} :

$$Signal = N_{+-}^{meas} - CB = N_{+-}^{meas} - 2\sqrt{N_{++}^{meas} N_{--}^{meas}} \frac{A_{+-}}{\sqrt{A_{++} A_{--}}} \qquad [10]$$

Once the combinatorial background subtracted, the invariant mass spectrum will in addition to the direct decay of the vector mesons, still contain broad contributions from Dalitz decays. One has to understand and calculate all possible channels contributing to the di-lepton spectrum.

All potential sources of di-leptons ("the cocktail")

The background-subtracted di-lepton invariant mass spectrum still contains broad continuum due to Dalitz decays of resonances and mesons (Table 3). In order to extract the vector-meson signal, the measured invariant mass spectrum is compared with the "hadronic cocktail", which contains all known sources of lepton pairs produced in the detector acceptance. Any excess or lack of strength can then be an indication of possible medium modifications.

i	Dilepton channel	
1	Dalitz decay of π^0:	$\pi^0 \to \gamma e^+ e^-$
2	Dalitz decay of η:	$\eta \to \gamma e^+ e^-$ (or $\mu^+\mu^-$)
3	Dalitz decay of ω:	$\omega \to \pi^0 e^+ e^-$
4	Dalitz decay of Δ:	$\Delta \to N e^+ e^-$
5	direct decay of ω:	$\omega \to e^+ e^-$
6	direct decay of ρ:	$\rho \to e^+ e^-$
7	direct decay of ϕ:	$\phi \to e^+ e^-$
8	direct decay of J/Ψ:	$J/\Psi \to e^+ e^-$
9	direct decay of Ψ':	$\Psi' \to e^+ e^-$
10	Dalitz decay of η':	$\eta' \to \gamma e^+ e^-$
11	pn bremsstrahlung:	$pn \to pne^+e^-$
12	$\pi^\pm N$ bremsstrahlung:	$\pi^\pm N \to \pi N e^+ e^-$, where $N = p$ or n

Table 3: Different di-lepton channels

There are many transport codes that can be used to calculate the "cocktail" specific to one's experiment. The predictions are filtered through the acceptance of the detector before comparing to data. Some of these transport codes are available on the web and can be downloaded: the Hadron-String Dynamics (HSD)[49] code, the Ultra relativistic Quantum Molecular Dynamics (UrQMD)[50] code, the Nantes' Isospin-QMD (IQMD)[51] code, and the Giessen Boltzmann-Ühling-Uhlenbeck (GiBUU)[52] code.

Figure 33 show the GiBUU cocktail predictions for $^{208}Pb(\gamma, e^+e^-)X$ reaction with E_γ = 2.2 GeV.[53] In these calculations, the hadronic nature of the incoming photon, shadowing,

Pauli blocking, all nuclear resonances, the in-medium propagation of produced particles out of nuclear volume (self-energies, widths) are included. In the first step, the incoming photons react with a single nucleon taking into account the effects of shadowing. Then in the second step, the produced particles are propagated explicitly through the nucleus allowing for final-state interactions, governed by the semi-classical BUU transport equations. Final state interactions are explicitly treated (absorption, side-feeding by couple channel effects. Etc.)

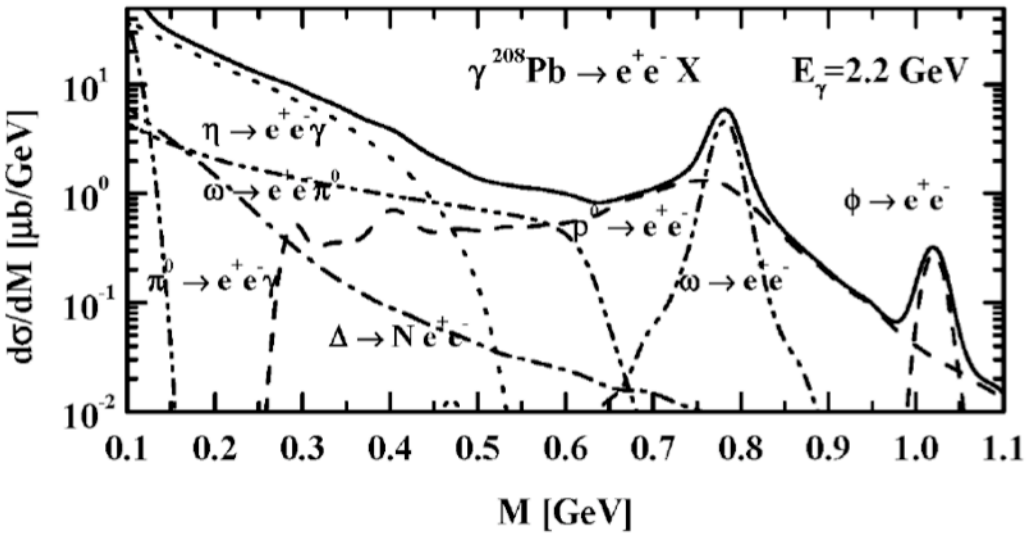

Figure 33: GiBUU predictions for e+e- invariant mass spectrum photo-produced on Pb.

Vector mesons in Heavy Ion Reactions:

The first experimental results suggesting possible medium modifications of the ρ-meson came from relativistic heavy-ion experiments. The CERES collaboration[54] (NA45) at CERN has studied the low e^+e^- invariant mass region up to ~1.5 GeV/c^2 in p+Be, p+Au, S+Au with with a mass resolution of Δm/m ~7%. They reported an excess in the e^+e^- mass spectrum in

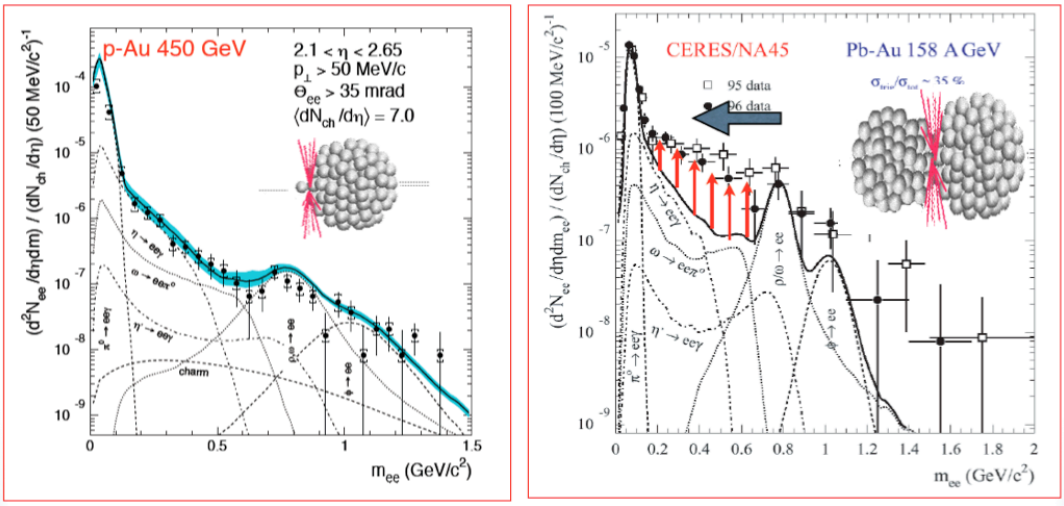

Figure 34: CERES (NA45) experiment at CERN. No excess yield observed compared to the cocktail in the in the p-Au reaction (left). Large excess observed in Pb-Au reaction (right).

the ρ-meson region. The experiment was a comparison of the mass spectrum from the *p*-Au reaction to the mass spectrum from the *Pb*-Au reaction. The data from the proton-induced reaction were described well by incorporating a cocktail of hadronic decay

channels into their analysis. In the CERES work, the heavy-ion collision data displayed an enhancement in the mass range between 300 and 700 MeV (Fig 34). This result could be explained as a temperature-induced decrease in the mass of the ρ meson.[55]
A second CERES measurement [56] with improved mass resolution (Δm/m ~2% at ρ –mass) confirmed the previous result however seem to favor a broadening of the ρ-meson rather than a simple mass shift (Fig 35).

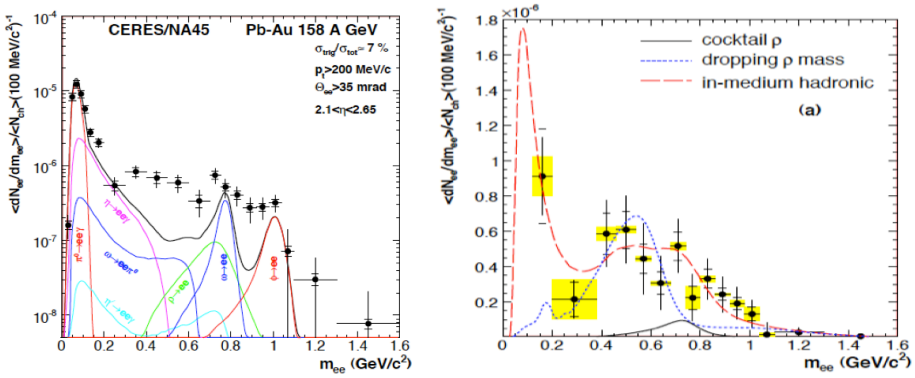

Figure 35: New analysis of CERES data. The excess yield over the cocktail is confirmed (left). The ρ-meson yield left after subtracting all other channels favors widening over simple mass shift.

Also at the CERN-SPS, the HELIOS/3 collaboration [57] studied the di-muon mass spectrum up to the J/Ψ mass with proton and sulfur beams on a tungsten target. They observed an excess in the di-muon mass spectrum below the ϕ-meson mass with the S-W reaction as compared with the p-W reaction. Recently , the NA60 collaboration [58] was able to extract the ρ-meson invariant mass spectrum and has reported a doubling of the ρ-meson width from their di-muon measurement from In-In collisions with no change in the ρ mass. This result confirm the predictions of Rapp and Wambach.[59]. Recent publications from the NA60 collaboration [60] confirm the earlier result (Fig 36).

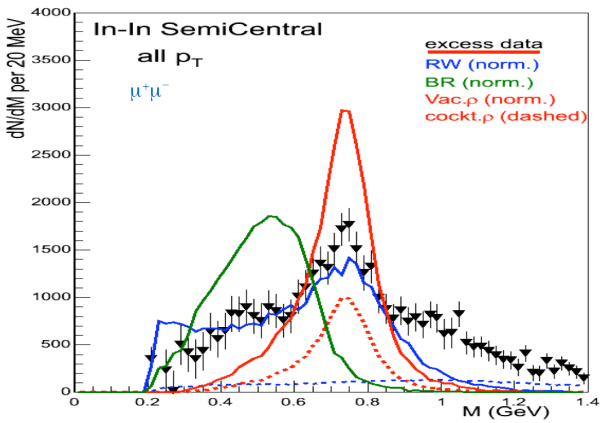

Figure 36: ρ-meson mass spectrum measured in the NA60 experiment.

There are many other heavy ion experiments that are not covered in this lecture such as DLS experiment at the BEVALAC[61], the HADES experiment at GSI[62], and the PHENIX experiment at RHIC[63]. What seems to come out from the heavy ion experiments is that the ρ-meson is modified in the medium. The modification seems to rather be a substantial broadening à la Rapp-Wambach rather than a simple downward mass shift à la Brown-Rho or Hatsuda-Lee.
However, one should note that in A+A collisions, the results are integrated over a whole range of ρ and T. Many stages are involved in these complicated reactions, the interpretation of the results is complicated because the reaction occurs in a non-equilibrium state before proceeding to equilibrium, while theoretical models predict the hadronic properties at equilibrium (normal nuclear density and zero temperature). The medium modifications of the ρ, ω, and ϕ mesons are predicted to be large enough to be observed in elementary reactions with hadron and photon beams.

Vector mesons in Nuclei (T=0 and $\rho \sim \rho_0$)

The vector mesons are produced in nuclei with simple probes such as γ,π,p that leave the nucleus in almost an equilibrium state [probe + A ➔V X ➔e^+e^-X]. The subsequent decay of the vector mesons in di-leptons is measured ad the invariant mass spectrum is calculated (Fig. 37).

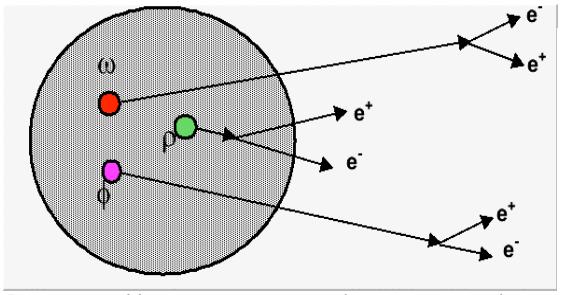

$$m_{\rho,\omega,\phi}(\vec{p},\rho,T) = \sqrt{(P_{e^+} + P_{e-})^2}$$

m : invariant mass of meson
P : 4-momentum of lepton
p: 3-momentum of meson/medium

Figure 37: Vector meson production in nuclei with subsequent decay in di-leptons.

Table 4 lists most of the "elementary reaction" experiments studying the vector mesons in nuclei. Experiments looking at other decay channels beside the di-lepton are also listed.

Experiment	*Reactions*	*Reference*
TAGX	γ +^{3}He-->ρ+X (ρ->$\pi^+\pi^-$)	64,65
KEK	p+A->ρ,ω,ϕ+X (ρ,ω->e^+e^-)	67,68
KEK	p+A->ϕ+X (ϕ->e^+e^-)	69
SPring-8	γ + A--> ϕ +A*(ϕ --> K^+K^-)	85
CBELSA-TAPS	γ+A--> ω +X (ω --> $\pi^0\gamma$)	70,82
JLab-g7a	γ+A-->(ρ,ω, ϕ)+A* (VM-->e^+e^-)	77,78
HADES	p+p,d->ρ,ω, ϕ +X (ρ,ω,ϕ ->e^+e^-)	62

Table 4: List of elementary reaction experiments. (Not exhaustive list). Not all experiments look at di-leptons in the final state

One of the first experiments to report medium modification of the ρ-meson was the TAGX collaboration that reported a large decrease of the ρ-meson mass in the reaction ^{3}He($\gamma, \pi^+\pi^-$)X, where the pion pairs result from sub-threshold ρ-meson production and decay.[64] The $\pi^+\pi^-$ mass spectrum was fit with ``non-ρ'' processes, a medium-modified ρ process, and a ρ process that is not modified by the medium. The best fits were consistent with the 20% reduction predicted by Brown-Rho scaling.[21] A second analysis based on the longitudinal polarization of the ρ mesons reported a smaller but significant decrease in mass.[65] Why TAGX observes such a large effect only in ^{3}He is not yet understood. These results are questionable given the small density of the nucleus and the final-state interactions on the pion pairs.

The experiment E325 at the KEK 12 GeV Proton Synchrotron was the first to measure di-leptons in search for the modication of the vector meson mass in a nucleus in elementary reactions. They measured the invariant mass spectra of e^+e^- pairs produced in 12 GeV proton-induced nuclear reactions. The two-arm spectrometer was designed to measure the decays of the vector mesons into e^+e^- as well as $\varphi \rightarrow K^+K^-$. The trigger was however not set to measure same charge pairs thereby precluding the possibility of normalizing the combinatorial background to the like-sign pair distribution (described earlier).
The combinatorial background shape was obtained by the event-mixing method, and its normalization was obtained by fitting the data together with contributions from $\omega \rightarrow e^+e^-$,

$\rho \rightarrow e^+e^-$, $\varphi \rightarrow e^+e^-$, $\eta \rightarrow e^+e^-\gamma$ and $\omega \rightarrow e^+e^-\pi^0$. The cocktail was obtained using the nuclear cascade code JAM.[66]

Figure 38 shows (on the left) the di-lepton invariant mass spectra measured on C and Cu and the background subtracted spectra (on the right) with the best fit results.[67,68,69]

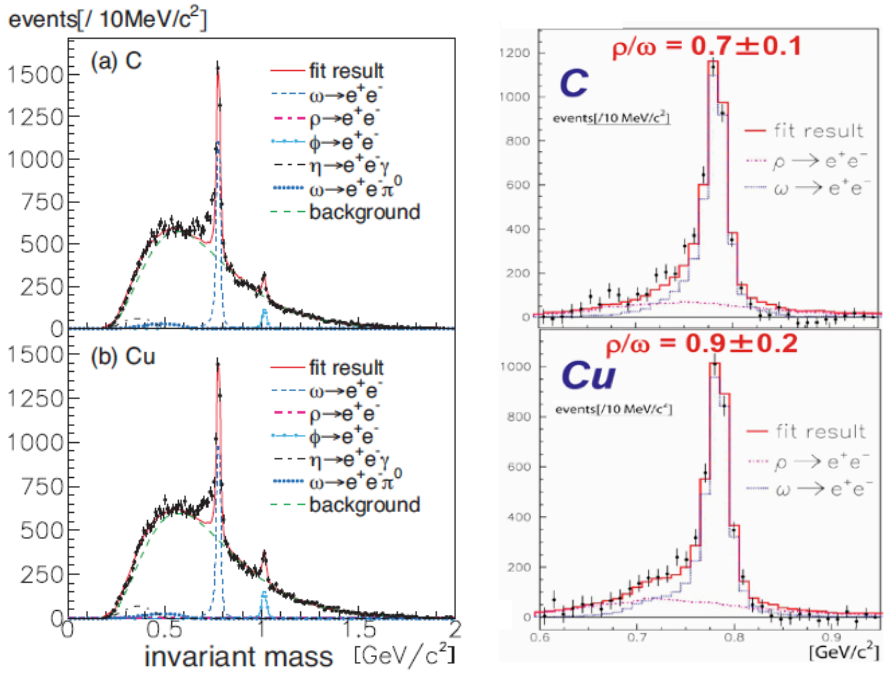

Figure 38: KEK E325 results on C and Cu

The best fit is obtained for a downward mass shift of 9.2 ± 0.2 % and no change in the widths of the ρ and ω mesons.

The ϕ-meson is a well defined narrow peak and the combinatorial background is not a main issue. When selecting "slow moving" ϕs a shoulder to the main ϕ peak appears and it is interpreted as corresponding to ϕ s decaying in the medium (Fig 39). A fit of the ϕ –peak in terms of two components, ϕ decaying outside the nucleus and ϕ decaying inside the nucleus, leads to a downward mass shift of 3.4 ± 0.6% of the mass and an increase of a factor 3-4 of the width of the ϕ.

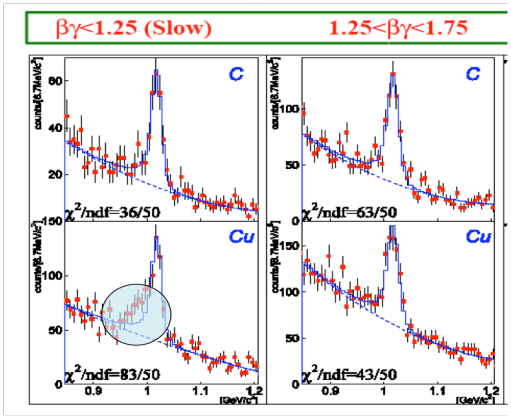

Figure 39: ϕ meson in KEK-E325

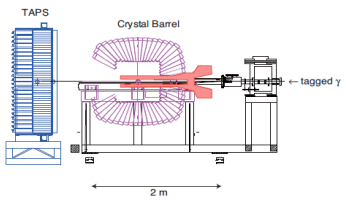

Figure 40: CBELSA_TAPS set-up.

The CBELSA/TAPS collaboration at the electron stretcher accelerator (ELSA) in Bonn used the $\gamma A \rightarrow \pi^0\gamma X$ reaction to study the ω meson in-medium behavior using the Crystal Barrel (CB) and TAPS crystal spectrometers (Fig. 40). Tagged photons in the energy range of 0.64–2.53 GeV were incident on targets (Nb and LH_2).
The branching ratio for $\omega \rightarrow \pi^0\gamma$ decay is the order of 9%. This channel provides a clean and exclusive mode to

study the ω in-medium properties. The ρ is highly suppressed since the $\rho \rightarrow \pi^0\gamma$ branching ratio < 10^{-3}.

However, a serious disadvantage is the possible strong final-stage interactions of the π^0 meson within the nucleus. The $\pi^0\gamma$ events are reconstructed from three photons and the invariant mass spectra is calculated as described in figure 41.

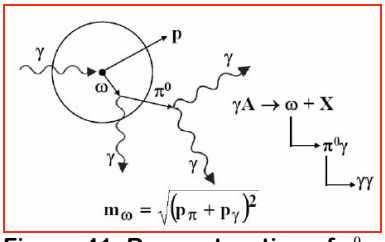

Figure 41: Reconstruction of $\pi^0\gamma$ events from 3 γ.

In order to maximize the in nucleus decay probability, slow-moving ω-mesons with $|p_\omega| < 0.5$ GeV/c were selected. The large combinatorial background is due to four-photon decays of $\pi^0\pi^0$ and $\pi^0\eta$ where one of the four photons is missed. In a first analysis, a smooth polynomial background was assumed and was subtracted, and the resultant LH2 and Nb data are compared in the left panel of figure 42. A shoulder on the low-mass side of the ω peak was found in the Nb target and was interpreted as medium modified ω-mesons with a downward mass shift of 14%.[70]

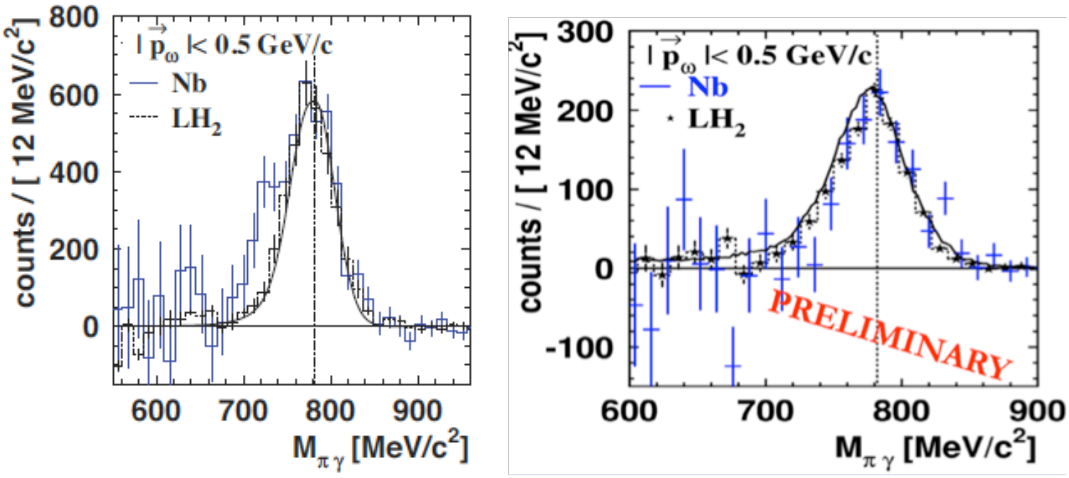

Figure 42: CBELSA-TAPS results. Previous analysis shows a shoulder interpreted as modified ω-mesons (left). New preliminary results shows no evidence of a shoulder(right).

The background-subtraction procedure was criticized by the Valencia group[71] pointing out that the observed shoulder was highly dependent on the shape of the background. In a reanalysis of the data, the CBELSA/TAPS group used the event-mixing technique to generate the background distribution, instead of using a polynomial function. The new preliminary results are shown in the right panel of figure 42 and there is no shoulder anymore.[72] The results are compatible with no mass shift. Therefore, until the reanalysis is finalized by the group, the ω in medium studies in this channel should be considered as inconclusive. High statistics data measured at MAMI is being analyzed to check these recent findings.

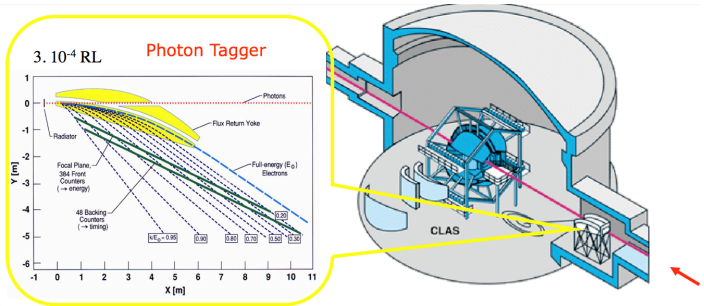

Figure 43: JLab Hall B Tagger

The J-Lab E01-112 experiment (also know as CLAS experiment g7a) was conducted in Hall B at the Thomas Jefferson National Accelerator Facility (TJNAF). An electron beam that was accelerated by the Continuous Electron Beam Accelerator Facility (CEBAF)[73] to an energy of 3 or 4 GeV was directed into Hall B. The beam was incident on a radiator with a 10^{-4} radiation

length thickness and deflected into the Hall B photon tagging facility.[74] The outgoing bremsstrahlung photon beam was reduced with a 1 mm-aperture collimator such that the beam-spot size on the target was 1 cm. The incident tagged-photon flux on target was approximately $5x10^7$ photons/s over an energy range from 0.61 GeV to 3.82 GeV. The vector mesons were photo-produced on LD_2, C, Fe, Ti and Pb. A multi-segmented target consisting of a liquid deuterium (LD2) cell and seven solid foils, each with a 1.2 cm diameter, was used (Fig. 44). The outgoing vector mesons were reconstructed from their decay to e^+e^- pairs. The leptons were detected with the Electromagnetic Calorimeters (EC) and Cerenkov Counters (CC) of the CLAS detector.[34]

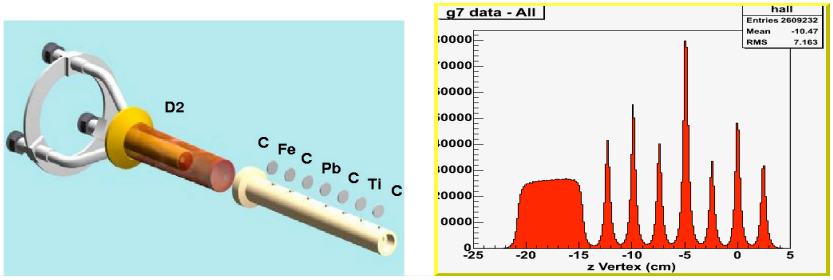

Figure 44: Multi-segmented target (left). Reconstructed vertex from e^+ e^- pairs.

The CLAS detector is ideal for this experiment owing to its ability to detect multi-particle final states and its high e/π rejection factor. Effective discrimination between lepton and pion pairs to the level of 10^{-7} are easily achieved.

After selecting e^+e^- pairs, we still have to deal with a background of random combinations of pairs due to the uncorrelated sources. The same-charge pairs method was successfully used to determine the combinatorial background (Fig. 45). Once the combinatorial background subtracted, all possible physics processes were simulated using a realistic model corrected for the CLAS acceptance. The events were generated using a code based on a semi-classical Boltzmann-Uehling-Uhlenbeck (BUU) transport model developed by the group of U. Mosel at the University of Giessen which treats the photon-nucleus reactions as a two-step process.[75] The shape of the narrow ω and ϕ vector mesons, and the ω Dalitz channel are well described by BUU model, and these distributions were fitted to the data, then subtracted, leaving just the experimental spectra of the ρ mass. The extracted ρ mass distributions are then fitted with the suggested functional form of $1/m^3$ times a Breit-Wigner function.[76]

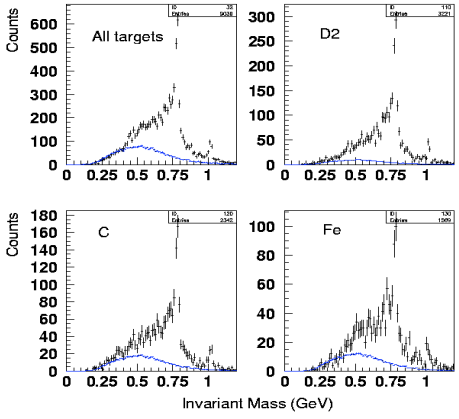

Figure 46: Combinatorial background (blue) determined by same charge pair method.

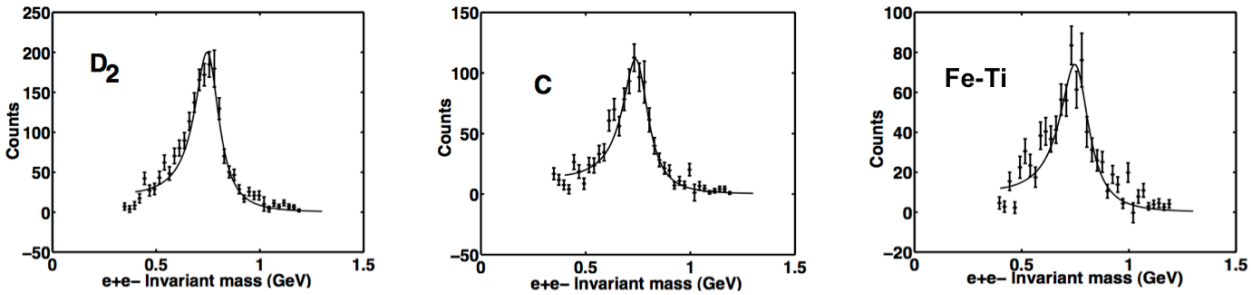

Figure 45: Extracted ρ mass spectra are fitted with the proper mass function.

The results of the fits are shown in figure 46 and tabulated in Table 5. The fits describe the data very well. The masses are consistent with the PDG values (no shift) and the widths are consistent with the collisional broadening ($\Delta\Gamma$~70 MeV in Fe)[77,78] and disagree with the KEK findings. On should note that the momentum of the vector mesons in this experiment are greater than 0.8 GeV/c.

Target	Mass (MeV/c^2) CLAS data	Width(MeV/c^2) CLAS data	Mass(MeV/c^2) Giessen BUU	Width(MeV/c^2) Giessen BUU
^{2}H	**770.3 +/- 3.2**	**185.2 +/- 8.6**	-	-
^{12}C	**762.5 +/- 3.7**	**176.4 +/- 9.5**	773.8 +/- 0.9	177.6 +/- 2.1
^{48}Ti-^{56}Fe	**779.0 +/- 5.7**	**217.7 +/- 14.5**	773.8 +/- 5.4	202.5 +/- 11.6

Table 5: Results of fits to the r-meson mass spectrum observed in the JLab g7 experiment compared to GiBUU predictions with no medium modifications.

In-medium width from transparency-ratio Measurements

When produced with large momenta, the ω and ϕ mesons (due to their longer lifetimes) will decay outside the nucleus and therefore be detected with properties of their free-space values. However, information on the in-medium width of these mesons can be extracted from their interactions with the nucleons as the mesons escape the nucleus using the transparency ratio T defined (for a vector meson V) as:

$$T_A = \frac{\sigma_{\gamma A \to VX}}{A \cdot \sigma_{\gamma N \to VX}} \qquad [11]$$

$\sigma\,\gamma_{A\to VX}$ is the inclusive nuclear vector-meson (V) photo-production cross section and $\sigma\,\gamma_{N\to VX}$ is cross section on a free nucleon. The transparency ratio T is a measure of the loss of vector-meson flux via inelastic processes in the nucleus, and is related to the absorptive part of the meson-nucleus potential. Extracting the in-medium meson width from the A dependence of the ratio T requires comparison with theoretical calculations. These medium effects are discussed in detail for the ω meson[79] and for the ϕ meson.[80]

Common to all of these calculations is the collisional broadening. The in-medium width is calculated to be $\Gamma = \Gamma_0 + \Gamma_{coll}$ where Γ_0 is the natural width in vacuum and Γ_{coll} is the width due to collisional broadening. Using the low-density theorem[81,50], Γ_{coll} has the following relationship $\Gamma_{coll} = \gamma\rho v\sigma^{*}_{VN}$ where γ is the Lorentz factor, ρ is the density, v is the velocity of the meson, and σ^{*}_{VN} is the meson-nucleon total cross section in the nucleus.
To eliminate the nucleon cross section in the analysis of the transparency, a ratio is made of the heavier target transparencies and the ^{12}C transparency as given by the equation:

$$T_{norm} = \frac{12 \cdot \sigma_{\gamma A \to \omega X}}{A \cdot \sigma_{\gamma\,^{12}C \to \omega X}} \qquad [12]$$

For the ω-meson measured in the JLab g7 experiment, the ratio T_{norm} has been calculated for the ^{2}H, C, Fe/Ti, and Pb and is compared to the TAPS data and theoretical calculations (Fig. 47). The transparency ratio decreases rapidly as a function of A, indicating a substantial increase in the in-medium width of the ω. The JLab ratios (red points) drop

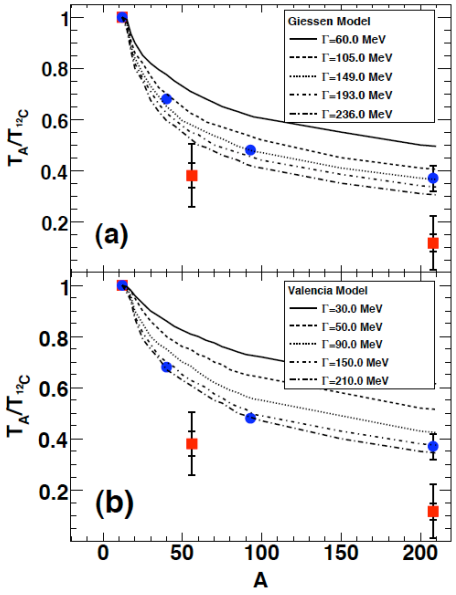

Figure 47: Transparency ratios from JLab (red) and TPAS (blue) compared to predictions (see text for details).

faster that the CBELSA-TAPS ratios (blue points) indicating an even larger in–medium width ($\Gamma_\omega \geq$ 200 MeV). The TAPS collaboration has published a value of Γ_w~130-150 MeV.[82] The experimental ratios are compared to theoretical predictions from the Giessen group[83] (top panel) and Valencia group[84] (bottom panel). The stronger ω-meson absorption observed in the e^+e^- channel cannot be explained with the current theoretical calculations.

ϕ-Meson absorption in nuclei

The photo-production of φ mesons from Li, C, Al and Cu targets has been measured at E_γ = 1.5 – 2.4 GeV at SPring-8 (LEPS), in the $\gamma A \rightarrow K^+K^-X$ channel.[85] Using a Glauber-type model calculation, the in-medium φ-nucleon cross section was deduced to be $\sigma_{\varphi N} = 37^{+17}_{-11} mb$, which is much larger than the free-space value used as an input in most model calculations. The transparency ratios (normalized to C) are shown in figure 48 and compared to preliminary JLab results and the Giessen theoretical predictions. The Jlab and the Spring8 results are compatible within statistical uncertainties and seem to indicate a width that can be as large as Γ_ϕ~ 70 MeV in the medium.

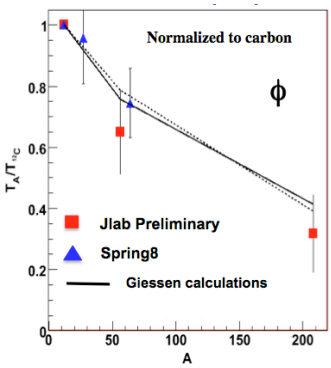

Figure 48: Transparency ratios for the ϕ-meson.

Table 6 summarizes all the results from the different experiments

exp	reaction	Momentum Acceptance	ρ	ω	ϕ
KEK	pA 12 GeV	p >0.6 GeV/c	(Δm/m)=-9% ΔΓ ~0	(Δm/m)=-9% ΔΓ ~0	(Δm/m)=-3.4% (Γ*/Γ) ~3.6
JLab	γA 0.6-3.8 GeV	p >0.8 GeV/c	Δm ~ 0 ΔΓ ~70 MeV (ρ~ρ_0/2)	ΔΓ(ρ_0) > 200 MeV <p_ω> >1 GeV/c	Compatible with Spring8
TAPS	γA 0.9-2.2 GeV	p >0 MeV/c	NA	Δm ~ 0 p_ω<0.5 GeV/c ΔΓ(ρ_0) ~ 130 MeV <p_ω> = 1.1 GeV/c	NA
Spring8	γA 1.5-2.4 GeV	p >1.0 GeV/c	NA	NA	ΔΓ(ρ_0) ~ 70 MeV <p_ϕ> = 1.8 GeV/c
CERES	Pb+Au 158 AGeV	p_t >0 GeV/c	Broadening favored over mass shift	NA	NA
NA60	In+In 158 AGeV	p_t >0 GeV/c	Δm ~ 0 Strong broadening	NA	NA

Table 6: Experimental results on the in-medium mass and width of the ρ, ω and ϕ mesons measured in different experiments.

VI. SUMMARY AND CONCLUSIONS

The study of the modifications of the properties of hadrons in the medium is one of the main topic of research in hadronic physics. The many ongoing theoretical and experimental studies attest to the vibrancy of this field. QCD is the fundamental theory of the strong interactions and a lot of progress has been achieved in trying to describe nuclear and hadronic physics in terms of the fundamental degrees of freedom (quarks and gluons). However, a number of open questions still remains, effective theories and ultimately LQCD will provide a deeper and more quantitative understanding of QCD in the non-perturbative regime.

The dynamical breaking of chiral symmetry realized in the QCD vacuum endows the hadrons with mass. The chiral condensate $<0|q\bar{q}|0>$ is the order parameter measuring the breaking of chiral symmetry and its study is as important as the search for the Higgs to understand the origin of the mass of hadrons. The quark condensate is predicted to change in hot and/or dense medium as a function of temperature T and density ρ. LQCD predicts that at high T and/or ρ , the quark condensate should vanish and chiral symmetry should be restored. In ordinary nuclear matter, the value of the quark condensate is predicted to drop by 35% indicating a partial restoration of chiral symmetry. Linking the quark condensate to actual observables is not an easy task, only in the case of low energy pions such a relation has been established. QCD based models provide constraints for hadronic models and predict changes for average properties such as the mass of hadrons. Hadronic models calculate the spectral function of the hadrons in the medium providing more information that just the mass. However, linking the spectral function to actual observed mass spectra is not straightforward and is model dependent.

In this lecture, we have covered a lot of experiments and the question that remains is: Do we have any strong evidence for partial restoration of chiral symmetry?

The strongest evidence comes from deeply bound pionic states where the results suggest an in-medium drop of the πN isovector scattering length b_1 which indicates a 33% drop of $|<0|q\bar{q}|0>|$ in normal nuclear matter. These conclusions are consistent with those derived from low energy pion elastic scattering.

The 2π enhancement in the σ channel (I=o, J=0) near the $2m_\pi$ threshold that is predicted is chiral symmetry is partially restored is indeed observed in several experiments. However as long as the enhancement can also be explained by final state interactions no unambiguous conclusions can be drawn from these studies.

The kaon-nucleon interaction in the medium seem to be modified. A repulsive KN potential of 20 ± 5 MeV at normal nuclear density is required to explains the FOPI and ANKE results.

The study of the in-medium properties of light vector mesons (ρ, ω and ϕ) is interesting because of their leptonic decay channel. Di-lepton has negligible final state interaction and leave the hadronic medium with no distortions providing "a clean tool to look into the medium". Experiments looking at the di-lepton decay of the vector mesons range from heavy-ion collisions to elementary reactions with γ, π and p. They all have developed state of the art lepton identification and are able to accurately estimate the huge combinatorial background.

In all heavy-ion reactions, an excess of di-leptons is observed in the region of the light vector mesons. This excess can be explained by a substantial widening of the ρ with no mass shift. Several elementary reactions experiments have report medium modifications for the ρ, the ω and the ϕ. Table 6 summarizes the experimental situation for the light vector mesons. A broadening in the nuclear medium has been reported by almost all experiments. For the ρ meson quantitative agreement between theory and experiment has been achieved while for the ω and φ meson the broadening deduced from transparency-ratio measurements is a factor 2-3 larger than predicted theoretically. The majority of experiments does not find evidence for mass shifts in the medium. For the ρ meson only one experiment (KEK) reports a drop of 9% in mass. Looking for in-medium mass shifts

turns out to be more complicated than initially thought because of the observed large in-medium broadening. The ρ meson has already a large width in vacuum and in the medium its width is broadened by an additional factor of about 1.5-3. Speaking of mass shift versus width broadening doesn't make much sense. The ω and φ meson are narrow in vacuum but are found to widen by a factor of the order of 15 in nuclear matter. This drastically reduces the branching ratio for in-medium decays into the channels of interest (di-leptons, $\pi^0\gamma$,..), making these experiments less sensitive to a direct observation of medium modifications. The latest models predict that most of the medium modifications happen when the meson have momenta less than 0.7 GeV/c with respect to the medium (Figure 49). Next generation experiments with much higher statistics and improved acceptance for low momenta mesons are needed to obtain reliable results. Several experiments are planned. Experiment g7b (E-08-018) at JLab[86] will look at the momentum dependence of the medium modifications of the ρ, ω and φ-mesons. At JPARC in Japan, in addition to several experiments planned to study mesic atoms, two experiments will continue to study the ρ, ω and φ-mesons with an upgraded version of the KEK E325 detector. Heavy-ion reactions at HADES, RHIC, FAIR and CERN will continue to study the effect of the medium on hadrons. They will extend the current studies to the charm sector.

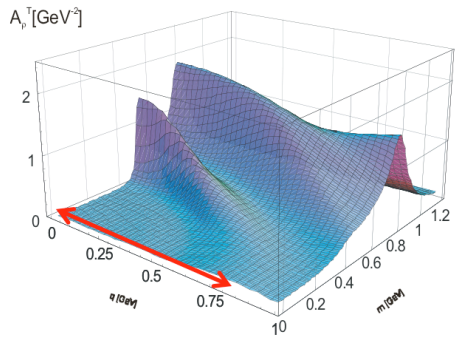

Figure 49: Spectral function of the ρ-meson at a function of in-medium momentum

During the next decade, substantial theoretical and experimental efforts will continue to be being carried out in this very active field.

ACKNOWLEDGMENTS

I would like to thank the organizers of the 2009 Ecole Internationale Joliot Curie for a wonderful meeting.

REFERENCES

[1] P.W. Higgs, Phys. Lett. 12 (1964) 132
P.W. Higgs, Phys. Rev. Lett. 13 (1964) 508
[2] Y. Nambu and G. Jona-Lasinio, Phys. Rev. 122 (1961) 345
Y. Nambu and G. Jona-Lasinio, Phys. Rev. 124 (1961) 246
[3] 2004 Nobel Lectures in Physics.
[4] Lord Kelvin, Baltimore Lectures, 1884.
[5] The Particle Data Group, Amsler, C., et al., Physics Letters B667 (2008) 1.
[6] P. O. Bowman et al, Phys. Rev. D71(2005)054507.
[7] For the ALEPH COLLABORATION arXiv :hep-ex/0506072v1 (2005).
[8] M. Gell-Mann, R. Oakes and J. Renner, Phys. Rev. 175 (1968) 2195.
[9] T. Hatsuda et al, Phys. Rev. Lett. 55 (1985)158;
W. Weise et al, Nuc. PHys. A 553 (1993)59.
[10] C. Ratti et al, Phys. Rev. D73 (2006)014019 ;
S. Klimt et al, Phys. Lett. B249 (1990)386.
[11] P. Gerber et al, Nucl. Phys. B 321 (1989) 387;
T. D. Cohen etal, Phys. Rev. C 45 (1992) 1881;
H. Fujii et al, Phys. Lett. B 357(1995)199.
[12] J. Alam, et al, Annals Phys. 286 (2001) 159.
[13] W. Cassing et al, Phys. Rep. 308 (1999) 65.
[14] R. Rapp et al, Adv. Nucl. Phys 25 (2000) 1.
[15] R. S. Hayano and T. Hatsuda, arXiv:0812.1702v2 [nucl-ex].
[16] Y. Nambu, G. Jona-Lasinio, Phys. Rev. 122 (1961) 345.

Y. Nambu, G. Jona-Lasinio, Phys. Rev. 124 (1961) 246.
[17] T. Hatsuda, T. Kunihiro, Phys. Rev. Lett. 55 (1985) 158.
T. Hatsuda, T. Kunihiro, Phys. Lett. B185 (1987) 304.
[18] V. Bernard, U.G. Meissner, I. Zahed, Phys. Rev. Lett. 59 (1987) 966.
V. Bernard and U.G. Meissner, Phys. Rev. D38 (1988) 1551.
V. Bernard and U.G. Meissner, Nucl. Phys. A489 (1988) 647.
[19] Y. Kwon et al, Phys. Rev. C78 (2008) 055.
[20] T. Hatsuda and S. H. Lee, Phys. Rev. C46 (1992) R34;
T. Hatsuda and S. H. Lee, Nucl. Phys. B394 (1993) 221.
[21] G. E. Brown and M. Rho, Phys. Rev. Lett. 66 (1991) 2720.
[22] M. Harada et al, Phys. Rev. D66 (2002) 016003 ;
M. Harada and C. Sasaki, Phys. Lett. B537 (2002) 280;
M. Harada and C. Sasaki, Phys. Rev. D73, (2006) 036001.
[23] K. Saito and A. W. Thomas, 1995, Phys. Rev. C51, 2757.
K. Saito et al., Phys. Rev. C55 (1997) 2637.
K. Saito et al., Prog. Part. Nucl. Phys. 58 (2007)1.
[24] R. Rapp et al., Eur. Phys. Jour. A6 (1999) 415;
B Friman et al., Nucl. Phys. A617 (1997) 496;
R. Rapp et al., Nucl. Phys. A617 (1997) 472;
D. Cabrera et al., Nucl. Phys. A705 (2002) 90;
M. Lutz et al. , Nucl. Phys. A 705 (2002) 431.
[25] Aouissat et al., Nucl. Phys. A581 (1995) 471;
T. Hatsuda et al., Phys. Rev. Lett. 82 (1999) 2840;
P. Schuck et al., Zeit. Fur Phys. A330 (1988) 119.
[26] C. T. A. M. De Laat et al., Phys. Lett. B162 (1985) 81.
[27] H. Toki and T. Yamazaki, Phys. Lett. B213 (1988) 129.
[28] M. Iwazaki et al., Physical Review C 43 (1991)1099.
[29] S. Hirenzaki et al., Phys. Rev. C44 (1991)2472.
[30] T. Yamazaki et al., Zeitschrift fur Physik A 355 (1996) 219.
[31] K. Suzuki et al., Phys. Rev. Lett. 92 (2004) 072302.
[32] D. Gotta et al., Precision Physics of Simple Atoms and Molecules , (2008)165.
H. Schroder et al., Eur. Phys. Journ. C21 (2001) 473.
[33] R. S. Hayano, Prog Theor Phys 168 (2007)565.
[34] D. H. Wright et al., Phys. Rev. C37 (1988) 1155.
[35] E. Friedman et al, Phys. Rev. Lett. 93 (2004) 122302.
[36] M. R. Pennington, Mod. Phys. Lett. A22 (2007) 1439.
[37] I. Caprini et al., Phys. Rev. Lett. 96 (2006) 132001.
H. Leutwyler et al., Leutwyler, H., 2008, AIP Conf. Proc. 1030 (2008) 46.
[38] For the CHAOS Collaboration: F. Bonutti et al., Phys. Rev. Lett. 77 (1996) 603.
For the CHAOS Collaboration: N. Grion et al., Nucl. Phys. A763 (2005) 80.
[39] A. Starostin et al., Phys. Rev. Lett. 85 (2000) 5539.
[40] J. G. Messchendorp[et al., Phys. Rev. Lett. 89 (2002) 222302.
V. Metag, Progress in Particle and Nuclear Physics 55 (2005)35.
[41] O. Buss et al, Eur. Phys. Journ. A32 (2007) 219.
[42] W. Weise, Nucl. Phys. A610 (1996) 35c;
G. Q. Li et al., Nucl. Phys. A625 (1997) 372.
[43] D. B. Kaplan and A. E. Nelson, Phys. Lett. B175 (1986) 57.
[44] K. Tsushima et al., Phys. Rev. C62 (2000) 064904.
[45] M. L. Benabderrahmane et al., Phys. Rev. Lett. 102 (2009) 182501.
[46] W. Cassing et al., Nucl. Phys. A614 (1997) 415.
W. Cassing and E. L. Bratkovskaya. Phys. Rep. 308 (1999)65.
[47] M. Buescher et al., Eur. Phys. J. A 22, (2004) 301.
[48] A. Adare et al., Phys. Lett. B670 (2009) 313.
[49] HSD code: http://th.physik.uni-frankfurt.de/~brat/hsd.html
[50] UrQMD, http://th.physik.uni-frankfurt.de/~urqmd/
[51] IQMD, http://www-subatech.in2p3.fr/~theo/qmd/
[52] GiBUU,http://gibuu.physik.uni-giessen.de/GiBUU
[53] M. Effenberger et al, Phys. Rev. C60 (1999) 044614.
[54] G Agakichiev et al., Phys. Rev. Lett. **75** (1995) 1272.
[55] G Q Li et al., Phys. Rev. Lett. **75** (1995) 4007.
[56] D. Adamová et al., arXiv:nucl-ex/0611022 v1 13.
[57] M Massera et al., Nucl. Phys. **A590** (1995) 93c.
[58] R Arnaldi et al., Phys. Rev. Lett. **96** (2006) 162302.
[59] R Rapp et al., Nucl. Phys. **A617** (1997) 472.
[60] S Damjanovic et al., Eur. Phys. J. **C49** (2007) 235.

S Damjanovic et al., Nucl. Phys. **A783** (2007) 327.
[61] G. Roche et al., **Phys. Rev. Lett. 61 (1988) 1069;**
R. J. Porter et al., **Phys. Rev. Lett. 79 (1997) 1229;**
C. Naudet et al., Phys. Rev.Lett. 62 (1989) 2652.
[62] P. Salabura et al., Progress in Particle and Nuclear Physics 53 (2004) 49.
[63] S. Afanasiev et al. (for the PHENIX Collaboration), eprint 0706.3034 (2007)
A. Toia, (for the PHENIX Collaboration), Nucl. Phys. A774 (2006) 743.
Toia, A. (for the PHENIX Collaboration), Eur. Phys. Jour. C 49, (2007) 243.
A. Toia, (for the PHENIX Collaboration), eprint 0805.0153 (2008).
[64] G. J. Lolos *et al., Phys. Rev. Lett.* **80** (1998) 241.
[65] G. M. Huber *et al., Phys. Rev.* **C68** (2003) 065202.
[66] Y. Nara et al., Phys. Rev. C 61 (1999) 024901.
[67] R. Muto et al., J. Phys, G: Nucl. Part. Phys. **30** (2004) S1023.
[68] R. Muto *et al., Phys. Rev. Lett.* **98** (2007) 042501.
[69] M Naruki *et al.*, *Phys. Rev. Lett.* **96** (2006) 092301.
[70] D. Trnka *et al.*, *Phys. Rev. Lett.* 94 (2005) 192303,.
[71] M. Kaskulov et al., Eur. Phys. Jour. A31 (2007) 245.
[72] V. Metag, private communication, (2009).
[73] . C W Leemann et al., Annu. Rev. Nucl. Part. Sci. **51** (2001) 413.
[74] D. Sober et al., Nucl. Inst. and Meth. **A440** (2000) 263.
[75] P Muehlich et al., arXiv:nucl-th/0210079 (2002).
[76] G. Q. Li et al., arXiv:nucl-th/9611037 v1 (1996);
M Effenberger et al., arXiv:nucl-th/9903026 v2. (1999);
H B O'Connell et al., Prog. Part. Nucl. Phys. **39**, (1997) 201.
[77] R. Nasseripour *et al.*, Phys. Rev. Lett. 99 (2007) 262302.
[78] M. H. Wood et al., Phys. Rev. C78 (2008) 015201.
[79] M. Kaskulov et al., Phys. Rev. **C75** (2007) 064616 .
[80] P. Muehlich and U. Mosel, Nucl. Phys. **A765** (2006) 188;
E. Oset and A. Ramos, Nucl. Phys. **A679**, (2001) 616;
D. Cabrera et al., Phys. Rev. **C67** (2003) 045203;
D. Cabrera et al., Nucl. Phys. **A733** (2004) 130;
V. K. Magas et al., Phys. Rev. **C71** (2005) 065202.
[81] C. B. Dover et al., Annals Phys. 66 (1971) 248.
[82] M. Kotulla et al., Phys. Rev. Lett. 100 (2008) 192302.
[83] P. Muehlich and U. Mosel, Nucl. Phys. **A773** (2006) 156.
[84] M. Kaskulov et al., Eur. Phys. J. A **31** (2007) 245.
[85] T. Ishikawa et al., Phys. Lett. B608 (2005) 215.
[86] M. Wood et al., http://www.jlab.org/exp_prog/proposals/08/PR-08-018.pdf